European Journal of Medicinal Chemistry 180 (2019) 224–237

Contents lists available at ScienceDirect

European Journal of Medicinal Chemistry

journal homepage: http://www.elsevier.com/locate/ejmech

Research paper

Antiproliferative activity of (*R*)-4′-methylklavuzon on hepatocellular carcinoma cells and EpCAM$^+$/CD133$^+$ cancer stem cells via SIRT1 and Exportin-1 (CRM1) inhibition

Murat Delman [a], Sanem Tercan Avcı [b, c], İsmail Akçok [d], Tuğçe Kanbur [d], Esra Erdal [b, c, **], Ali Çağır [d, *]

[a] Department of Biotechnology and Bioengineering, Izmir Institute of Technology, 35430, Urla, Izmir, Turkey
[b] Izmir Biomedicine and Genome Center, 35340, Balcova, Izmir, Turkey
[c] Department of Medical Biology and Genetics, Faculty of Medicine, Dokuz Eylul University, 35340, Balcova, Izmir, Turkey
[d] Department of Chemistry, Faculty of Science, Izmir Institute of Technology, 35430, Urla, Izmir, Turkey

ARTICLE INFO

Article history:
Received 6 May 2019
Received in revised form
7 July 2019
Accepted 8 July 2019
Available online 9 July 2019

Keywords:
Hepatocellular carcinoma
Cancer stem cell
SIRT1 inhibitor
CRM1 inhibitor
Topoisomerase I inhibitor
Klavuzon

ABSTRACT

Cytotoxic effects of (R)-4′-methylklavuzon were investigated on hepatocellular carcinoma cells (HuH-7 and HepG2) and HuH-7 EpCAM$^+$/CD133$^+$ cancer stem cells. IC_{50} of (R)-4′-methylklavuzon was found as 1.25 μM for HuH-7 parental cells while it was found as 2.50 μM for HuH-7 EpCAM$^+$/CD133$^+$ cancer stem cells. (R)-4′-methylklavuzon tended to show more efficient *in vitro* cytotoxicity with its lower IC_{50} values on hepatocellular carcinoma cell lines compared to its lead molecule, goniothalamin and FDA-approved drugs, sorafenib and regorafenib. Cell-based Sirtuin/HDAC enzyme activity measurements revealed that endogenous Sirtuin/HDAC enzymes were reduced by 40% compared to control. SIRT1 protein levels were upregulated indicating triggered DNA repair mechanism. p53 was overexpressed in HepG2 cells. (R)-4′-methylklavuzon inhibited CRM1 protein providing increased retention of p53 and RIOK2 protein in the nucleus. HuH-7 parental and EpCAM$^+$/CD133$^+$ cancer stem cell spheroids lost intact morphology. 3D HepG2 spheroid viabilities were decreased in a correlation with upregulation in p53 protein levels.

1. Introduction

Tumor recurrence and drug resistance in cancer therapy are major barriers to completely treat patients and save their lives. Some of the well-known chemotherapeutic agents are anthracyclines (doxorubicin, idarubicin, epirubicin, daunorubicin), taxanes (paclitaxel, docetaxel), camptothecin and its derivatives (topotecan, irinotecan), podophyllotoxin and its derivative (etoposide, teniposide), vinca alkaloids (vincristine, vinorelbine, vindesine, vinblastine) [1].

Styryl lactones are a member of these classes and low molecular weight phenolic secondary metabolites isolated from natural sources like genus *Goniothalamus*. Approximately 100 styryl lactones exist and some compounds act as immunosuppressive, antimycobacterial, antifungal, anti-inflammatory, insecticidal, antiplasmoidal [2–4], trypanocidal [5], and antifertility agents [6]. Styryl lactones were also reported to show effects of anti-tumor, teratogenic, pesticidal, embryotoxic activities [7].

Goniothalamin is one of the styryl lactones and exhibit cytotoxic and antiproliferative effects against several types of tumor cells [8]. Goniothalamin was shown to be cytotoxic against hepatocellular carcinoma [9], hepatoblastoma [10,11], HeLa cells [12,13], breast carcinomas, Jurkat cells, gastric, kidney cells [14–18] while it doesn't show cytotoxicity against normal cells and blood cells [1]. It was reported that antiproliferative ability of goniothalamin was explained with existence of Michael acceptor against cysteines and other nucleophiles [19–21].

Michael acceptors (soft electrophiles) specifically react with soft nucleophiles such as thiol group in molecules like glutathione (GSH) and cysteine amino acids [22–25].

FDA approved drugs; afatinib, ibrutinib, osimertinib proved the importance of unique cysteine targeting of a specific protein via irreversible hetero-Michael addition reaction as a next generation

* Corresponding author. Izmir Institute of Technology, Faculty of Science, Department of Chemistry, Gulbahce, Izmir, Turkey.
** Corresponding author. Izmir Biomedicine and Genome Center, 35340, Balcova, Izmir, Turkey.
E-mail addresses: esra.erdal@ibg.edu.tr (E. Erdal), alicagir@iyte.edu.tr (A. Çağır).

https://doi.org/10.1016/j.ejmech.2019.07.024
0223-5234/

approach for drug discovery.

Relationship of goniothalamin with sirtuin-1 (SIRT1) enzyme was shown via increased SIRT1 levels in IL-10 knock-out mice. SIRT1 is involved in TNF-α pathway and have ability to inhibit transcription factors, such as NF-κB and STAT-3, which increase pro-inflammatory responses followed by cancer progression, resulting in inhibition of inflammation [26,27].

Hepatocellular carcinoma (HCC) is the fifth most common cancer and second leading cause of cancer-related deaths worldwide. FDA approved drugs like sorafenib and regorafenib do not ameliorate the prognosis of the disease. HCC is characterized as highly aggressive type of tumor because of its heterogeneity, metastatic nature, poor prognose and drug resistance. The heterogeneity of tumor cells comes out as a result of the hierarchical organization of cancer stem cells (CSCs) [28]. So, besides conventional cytotoxic therapies targeting entire tumor cells in a non-selective manner, CSCs must be targeted for the efficient treatment of various types of cancer, including HCC [29].

Zheng et al. demonstrated that cells carrying surface markers, EpCAM, CD133, CD24, CD90, CD44, CD13, are thought to be HCC tumor initiating cells and have ability of differentiation, self-renewal and production of heterogeneous tumors. They revealed that cells with abovementioned surface markers are transcriptomically, phenotypically and functionally heterogeneous at the single-cell level. Besides this heterogeneity, they revealed that Triple$^+$ marker (EpCAM, CD133, CD24) phenotype is tumor specific compared to non-tumor tissue according to Liver Cancer Institute (LCI) and The Cancer Genome Atlas (TCGA) cohorts [30]. Most of the approved drugs do not target these kinds of tumor initiating cells which can form tumors from a very little number of cell populations.

Moreover, CD133$^+$ CSCs were resistant to chemotherapeutic agents such as doxorubicin and 5-fluorouracil as a result of upregulation of ATP-binding cassette (ABC) superfamily transporters [31]. Besides CD133$^+$ surface marker, Yamashita et al. demonstrated that EpCAM$^+$ HCC cells display hepatic cancer stem cell—like traits with self-renewal and differentiation ability and can initiate tumor from a very low number of cells in SCID mice [29].

It was shown that FDA-approved small molecules covalently bind to unique cysteine residues of certain proteins in various cancers. These small molecules can be listed as afatinib, (Cys797 of EGFR) for the treatment of metastatic non-small cell lung cancer (NSCLC); ibrutinib, (Cys481 of BTK) for B-cell malignancies; osimertinib, (Cys797 of EGFR T790 M mutant) for NSCLC; neratinib (Cys773 and Cys805 of EGFR and HER2$^+$) for breast cancer [32–38].

Our drug candidates, (*R*)-4′-methylklavuzon and TK126, which carry a Michael acceptor in their structures, are capable of targeting cysteine residues by making Michael addition reaction. Both drug candidates may act like acrylamide for cysteine residues. Previously, it was found that (*R*)-goniothalamin (1) and (*R*)-4′-methylklavuzon (2) are novel irreversible inhibitors of topoisomerase I [39]. Additionally, immunosuppressive effects of 4′-methylklavuzon was shown by inhibition of IL-2 production in T lymphocytes (Jurkat e6-1) with limited cytotoxicity [40]. Compound 3 (TK126) is also another klavuzon derivative and show remarkable cytotoxic activity over 3D spheroids of HuH-7 cell line (Fig. 1) [41].

Additionally, in house experiments revealed increased G1 and G2 arrests by (*R*)-4′-methylklavuzon in cancer cells directing us epigenetic modulators like class I/II histone deacetylases (HDACs) and sirtuins [41]. Specifically, SIRT1 and HDAC1 have roles in regulation of histones and non-histone proteins like p53. Moreover, structural similarity of (*R*)-4′-methylklavuzon and TK126 to goniothalamin which was shown to be CRM1 inhibitor, allowed us to test its CRM1 inhibitory properties in HCC cells for the first time in this study.

There have been several studies including antiproliferative activities of small molecules in various types of cancer cell lines via SIRT1 inhibition [42,43]. Up to date, there is no reported covalent inhibitor of SIRT1. On the other hand, it was demonstrated that 4-hydroxynonenal covalently binds to the Cys280 residue of SIRT3 by a Michael addition reaction. It was resulted in an allosteric inhibition of SIRT3 activity by disturbing the conformation of the zinc-binding domain [44]. Similarly, catalytic site of SIRT1 contains Zn^{2+} tetrathiolate subdomain which includes four surface exposed cysteine residues (Cys371, Cys374, Cys395, Cys398), conserved among all seven human sirtuins, to coordinate Zn^{2+} ion. It was also shown that, indirect effects like nitrosative/oxidative stress might also disrupt Zn^{2+} coordination by S-nitrosation of any cysteine residue resulting in complete inhibition of SIRT1 [45]. Hence, these cysteine residues of SIRT1 may also be an important target for klavuzon derivatives.

SIRT1 is a member of class III HDAC family which is NAD^+ dependent whereas class I/II HDAC families are zinc dependent for catalytic activity. SIRT1 has crucial roles in the maintenance of stemness as an epigenetic regulator. It is also speculated that CSCs and normal stem cells of the corresponding tissue include distinct stem cell networks which provides unique roles for sirtuins in CSCs [46]. Loss of SIRT1 provides reduced expression of CSC markers, decreased sphere formation and increased sensitivity to treatment. According to mutational analyses, only wild-type SIRT1 induces HCC cell proliferation and colony formation whereas mutation in deacetylase domain of SIRT1 deacetylase domain mutant doesn't induce the proliferation suggesting that HCC progression is maintained by deacetylation function of SIRT1 [47].

Li et al. showed that selective targeting of drug-resistant CSCs is possible by the inhibition of SIRT1 activity. In this study, elimination of imatinib-resistant CD34$^+$ chronic myeloid leukemia (CML) stem cells was achieved by *in vivo* treatment of Tenovin-6 (a small-molecule inhibitor of SIRT1 and SIRT2). This was basically a result of SIRT1 inhibition followed by the elevation of acetylated and total p53 levels [48].

It was found that SIRT1 is overexpressed in liver tumor cell lines (HuH7, HepG2, Hep3B, SKHep-1, HepKK1, HLF, HLE) in contrast to its very low levels in normal liver cells [49,50]. It was also demonstrated that *in vivo* inhibition of SIRT1 activity in HCC xenograft mice models reduces tumor growth. *In vivo* bioluminescent imaging showed that 80% of control mice developed tumors after day 11 whereas 33% of the mice that are SIRT1-knocked down developed tumors up to 30 days. All indicated HCC cell lines, regardless of their p53 status, HepG2 (wild-type), Hep3B (null) or HuH-7 (mutated) overexpress SIRT1 and their proliferations were reduced after SIRT1 inhibition [49].

CRM1 (exportin-1) causes aberrant export of tumor suppressors (p53, p73 and FOXO1), anti-apoptotic proteins (SIRT1, NPM and AP-1) and growth regulator/pro-inflammatory proteins (p21, p27, Rb, BRCA1, IkB and APC) from nucleus to cytosol in related cancer cells [51–53]. CRM1 was found to be overexpressed in HCC compared to non-tumorous liver tissue and specifically highly expressed in HCC subgroup (G3) which was identified by p53 mutations and overexpression of cell cycle regulating genes [54,55]. Overexpressed CRM1 causes inhibition of functional wild-type p53 by aberrant exportation from nucleus to cytoplasm [52]. Inhibition of CRM1 by small molecules like α,β-unsaturated δ-lactones is one of the therapeutic strategies in cancer research [56]. One of the cargo proteins of CRM1 is RIOK2 (right open reading frame 2) which is classified in RIO kinase family [57,58]. RIOK2 was found to be involved in the cell cycle regulation as a result of its phosphorylation by Polo-like kinase (PLK1) that functions in G2/M transition, spindle formation, chromosome congression and segregation, as well as cytokinesis by phosphorylating its specific substrates.

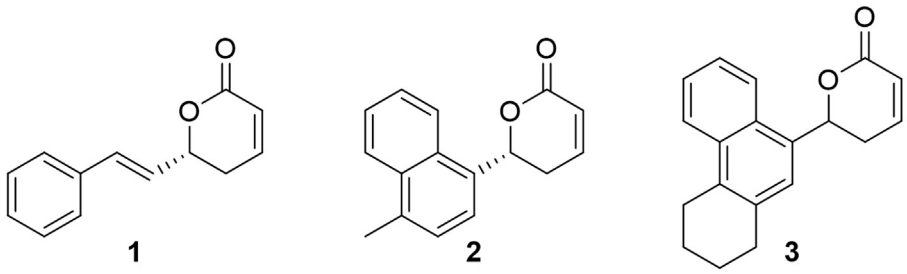

Fig. 1. Structures of (*R*)-goniothalamin (**1**), (*R*)-4′-methylklavuzon (**2**) and TK126 (**3**).

Prolonged mitotic exit was observed when RIOK2 was overexpressed whereas acceleration in mitotic progression was found when RIOK2 was silenced [59].

In this study, growth inhibitory effects of (*R*)-4′-methylklavuzon and its newly synthesized derivative, TK126 were tested on both hepatocellular carcinoma cell lines (HuH-7, HepG2) and EpCAM$^+$/CD133$^+$ cancer stem cells sorted from HuH-7. It was firstly demonstrated that (*R*)-4′-methylklavuzon causes cell cycle arrest by inhibiting endogenous SIRT1/HDAC and CRM1 activity in HuH-7.

2. Results and discussion

2.1. Synthesis of (R)-4′-methylklavuzon and TK126

Asymmetric synthesis of 4′-methylklavuzon (**2**) was performed starting from 4-methyl-1-naphthaldehyde (**4**) as summarized in Fig. 2. Simply, asymmetric allylation of aldehyde **4** was carried out by addition of allyltrimethoxysilane in the presence of (*R*)-Tol-BINAP.AgF catalyst developed by Yamamoto and coworkers to produce homoallylic alcohol **5** with 85% yield and 88% ee [60]. Then, treatment of produced alcohol with acryloyl chloride under basic condition gave acrylate ester **6** with 93% yield. Finally, Ist generation Grubbs' catalyst was used to perform ring closing metathesis reaction to produce the target klavuzon (**2**) with 69% yield [61].

Racemic synthesis of another klavuzon derivative, TK126 was performed according to the procedure reported in the literature [41].

2.2. (R)-4′-methylklavuzon inhibits proliferation of HuH-7 parental and EpCAM$^+$/CD133$^+$ cancer stem cells

To determine cytotoxic effects of drug candidate (*R*)-4′-methylklavuzon, we firstly performed MTT cell viability assay to identify IC$_{50}$ value. Based on the data, IC$_{50}$ values of (*R*)-4′-methylklavuzon on HuH-7 parental cells were determined as 10 μM for 24 h, 1.25 μM for 48 and 72 h while IC$_{50}$ values for EpCAM$^+$/CD133$^+$ cancer stem cells were determined as 10 μM for 24 h, 2.5 μM for 48 h and 1.25 μM for 72 h. So, CSCs were determined as more resistant against the drug candidate for 48 h compared to HuH-7 parental cells (Fig. 3A). IC$_{50}$ values for EpCAM$^-$/CD133$^-$ cells were similar as parental counterparts (Fig. S1A).

Furthermore, cell cycle analysis revealed a significant increase at G1 arrest in both parental and EpCAM$^+$/CD133$^+$ CSCs at low concentrations of 1.25 and 1.0 μM after 48 h of drug administration, respectively. Notably, only high concentration of drug (10 μM) results in significant increase at G2 arrest in HuH-7 parental cells after 48 h of drug administration (Fig. 3B). Similar results were obtained with EpCAM$^-$/CD133$^-$ cells as illustrated in Fig. S1A.

Significant increase at early apoptosis in HuH-7 parental cells at 10 μM was detected after 48 h of drug administration. No significant apoptotic effects were detected but dose-dependent increase in apoptosis was observed in EpCAM$^+$/CD133$^+$ CSCs (Fig. 3B). Apoptotic effects of (*R*)-4′-methylklavuzon on EpCAM$^-$/CD133$^-$ cells were found similar as illustrated in Fig. S1B.

When we analyzed the main regulators of cell cycle as CDK inhibitors, p21 and p27, we found that their expressions in HuH-7 parental cells were significantly upregulated at the intervals of 24, 48, 72 h after drug administration (Fig. 3C). p21 was also significantly upregulated in EpCAM$^+$/CD133$^+$ cancer stem cells after 72 h of treatment (Fig. 3C). Similar results related to p21 gene expressions were obtained in EpCAM$^-$/CD133$^-$ cells (Fig. S1B).

Conventional 2D microscopic analysis revealed that morphology and number of cells were significantly altered after drug administration as a consequence of cell cycle arrest and apoptosis (Fig. 3D). Similar alterations related to morphology and number of cells were obtained in EpCAM$^-$/CD133$^-$ cells (Fig. S1C).

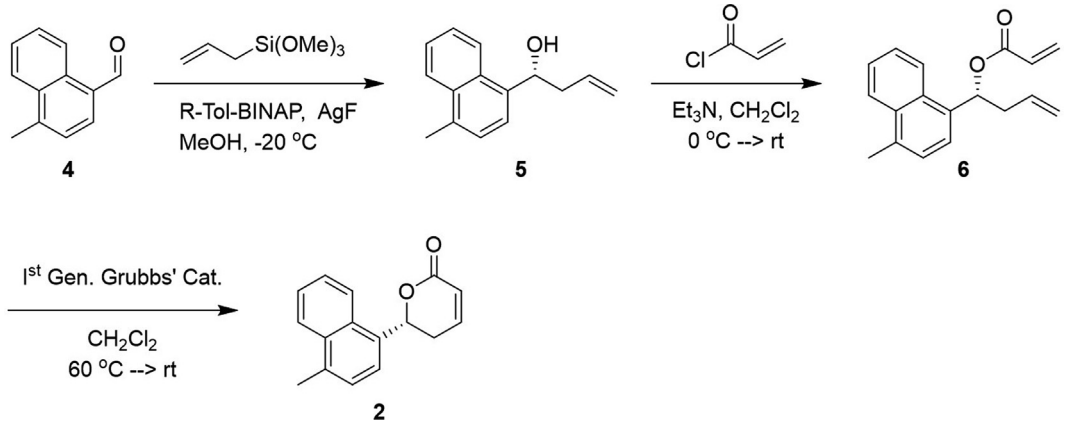

Fig. 2. Asymmetric synthesis of (*R*)-4′-methylklavuzon (**2**).

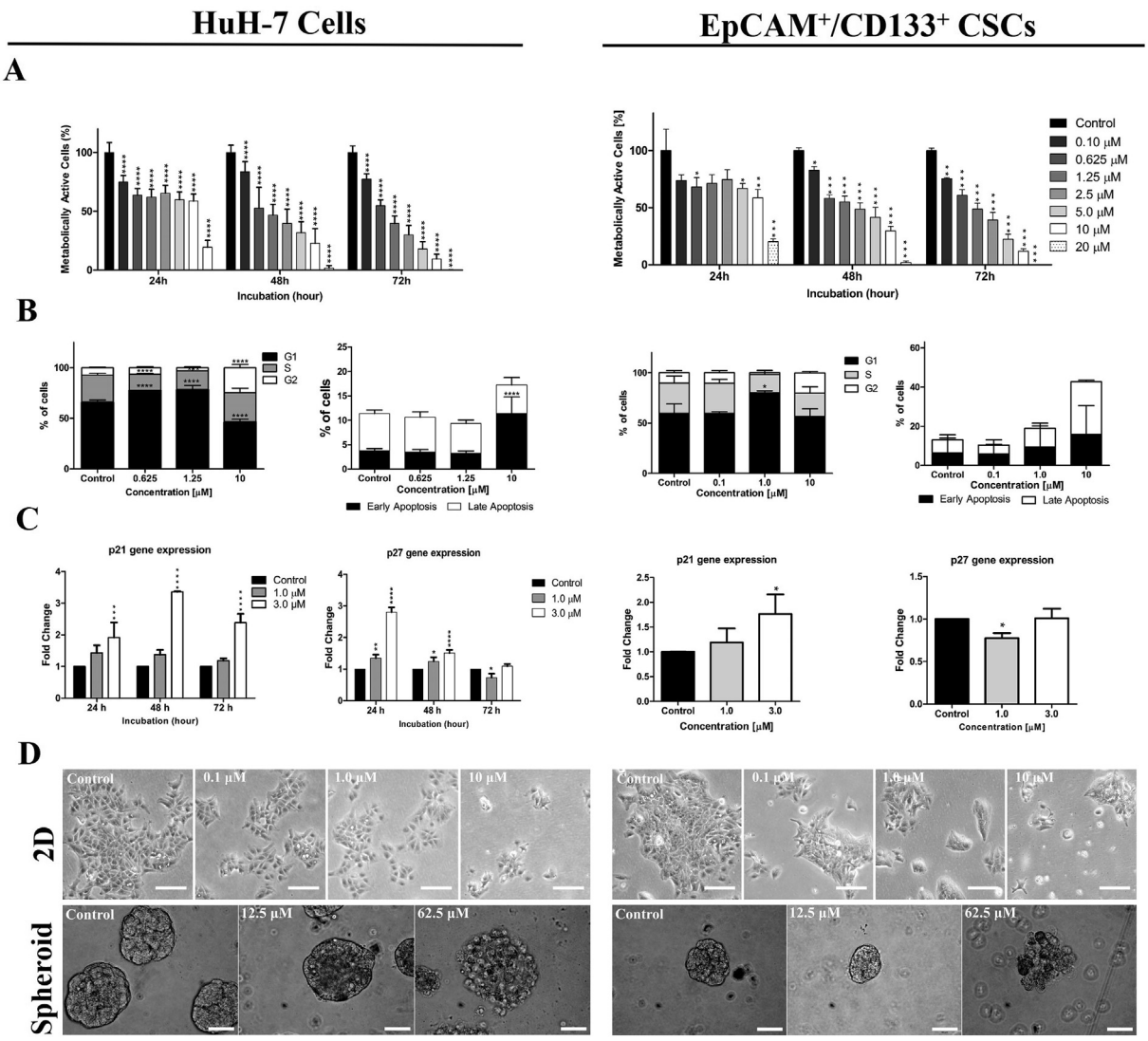

Fig. 3. A) Cytotoxicity analysis of HuH-7 parental and EpCAM$^+$/CD133$^+$ cancer stem cells, (**B**) Cell cycle analysis indicating G1 and G2 arrests in HuH-7 parental and EpCAM$^+$/CD133$^+$ cancer stem cells after 48 h, Apoptosis analysis showing increased early and late apoptosis in HuH-7 parental and EpCAM$^+$/CD133$^+$ cancer stem cells after 48 h, respectively. (**C**) Fold changes in p21 and p27 gene expressions in HuH-7 parental and EpCAM$^+$/CD133$^+$ cancer stem cells after 72 h, (**D**) Microscope images of 2D HuH-7 cells (10X) and 3D spheroids in matrigel (40X) formed with HuH-7 parental and EpCAM$^+$/CD133$^+$ cancer stem cells after 48 h of incubation with (*R*)-4′-methylklavuzon. Images were obtained by using 10X objective with 100 μm scale and 40X objective with 50 μm scale. Statistical analysis was performed with one-way ANOVA and p-values are <0.001 in ****, <0.001 in ***, <0.01 in ** and <0.05 in * indicating that results are statistically significant.

After (*R*)-4′-methylklavuzon treatment, HuH-7 parental and EpCAM$^+$/CD133$^+$ CSC 3D spheroids in matrigel became unhealthy and lost intact morphology at high doses of drug, especially at 62.5 μM concentration (Fig. 3D).

2.3. (R)-4′-methylklavuzon inhibits SIRT1 rather than class I/II HDAC enzymes in vitro

Importance of SIRT1 inhibition in selective targeting of drug-resistant cancer stem cells directed us to measure the effects of our drug candidate on SIRT1 activity. *In silico* docking of (*R*)-4′-methylklavuzon was performed by using Autodock Vina software [62] to verify spatial positioning of drug candidate in SIRT1 enzyme catalytic site (PDB ID: 4ZZI) [63]. We found that docking was spontaneous as it was revealed −9.4 kcal/mol as Gibbs free energy (Fig. 4A). Additionally, based on *in vitro* assay, (*R*)-4′-methylklavuzon inhibits SIRT1 enzyme activity in a dose dependent manner while it has no inhibitory effects on HDAC1 enzyme (Fig. 4A).

Cell-based assay revealed that Sirtuin/HDAC enzyme activity was reduced by 35–40% compared to control via drug administration at doses ranging from 0.10 to 5.0 μM and this significant decrease in enzyme activity remained constant at all doses after 24 h of drug administration. Notably, decrease in the enzymatic activity was consistent with the decrease in cell viability indicating the relationship between cytotoxicity of (*R*)-4′-methylklavuzon with Sirtuin/HDAC enzyme activity inhibition after 24 h. Furthermore, nuclear proteins containing class I/II HDAC enzymes that were isolated from HuH-7 parental cells were also tested with (*R*)-4′-methylklavuzon and no significant inhibition was achieved (Fig. 4B).

Similar results were obtained from EpCAM$^+$/CD133$^+$ CSCs with 32–39% of decrease in endogenous Sirtuin/HDAC enzyme activity and this decrement was correlated with a decrease in cell viability

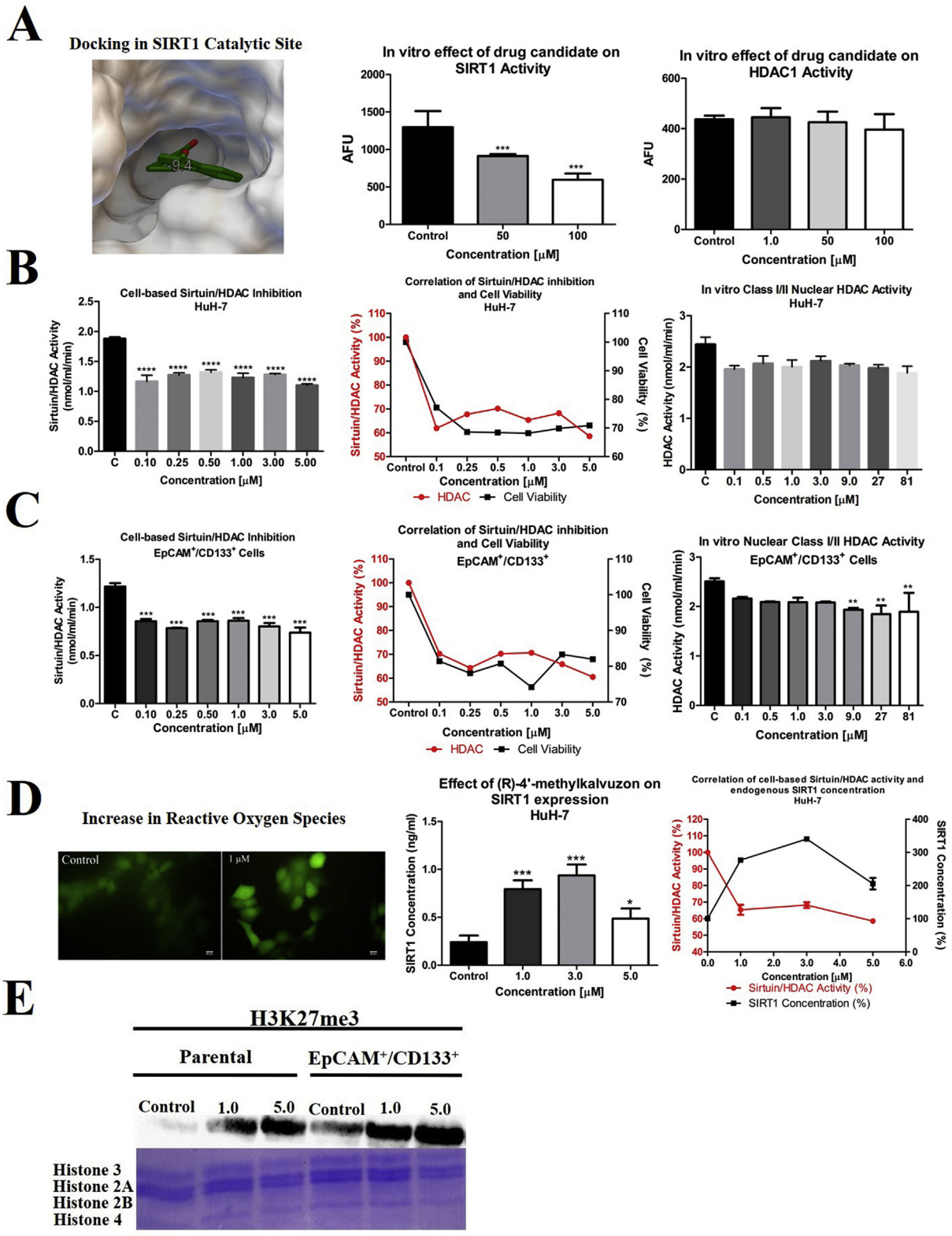

Fig. 4. (**A**) *In silico* analysis of (*R*)-4′-methylklavuzon docking in SIRT1 enzyme catalytic site, Inhibition of SIRT1 activity *in vitro*, Non-inhibitory effects of drug candidate on HDAC1 enzyme *in vitro*, **(B)** Inhibition of endogenous Sirtuin/HDAC activity in HuH-7 parental cells after 24 h, Correlation of endogenous Sirtuin/HDAC inhibition with HuH-7 parental cell viability after 24 h, Non-inhibitory effects of drug candidate on class I/II HDAC enzymes in nuclear extracts of HuH-7 parental cells after 24 h, (**C**) Inhibition of endogenous Sirtuin/HDAC activity in EpCAM^{+}/CD133^{+} cancer stem cells after 24 h, Correlation of endogenous Sirtuin/HDAC enzyme activity inhibition with EpCAM^{+}/CD133^{+} cancer stem cell viability after 24 h, Non-inhibitory effects of drug candidate on class I/II HDAC enzymes in nuclear extracts of EpCAM^{+}/CD133^{+} cancer stem cells after 24 h, **(D)** DCFDA staining of increased reactive oxygen species after 24 h of drug treatment, Upregulation of endogenous SIRT1 protein levels in HuH-7 parental cells after 24 h, Comparison of cell-based Sirtuin/HDAC enzyme activity inhibition with endogenous SIRT1 protein levels after drug administration, **(E)** Level of H3K27me3 modification increases in HuH-7 parental and EpCAM^{+}/CD133^{+} cancer stem cells. Statistical analysis was performed with one-way ANOVA using Dunnet's multiple comparisons test and p-values are <0.001 in ***, <0.01 in **, <0.05 in * and for SIRT1 ELISA data <0.003 in *** indicating that results are statistically significant.

after 24 h. Nuclear proteins containing class I/II HDAC enzymes that were isolated from EpCAM$^+$/CD133$^+$ cancer stem cells were also tested with (*R*)-4′-methylklavuzon and no significant inhibition was achieved (Fig. 4C). Similar effects of drug candidate on cell-based and *in vitro* HDAC enzyme activity in HuH-7 EpCAM$^-$/CD133$^-$ cells are illustrated in Fig. S2.

It was found that (*R*)-4′-methylklavuzon does not have significant inhibitory effects on HDAC1 enzyme activity *in vitro*. Data obtained from HDAC1 activity measurement is parallel to data obtained from *in vitro* class I/II histone deacetylase enzymatic activity measurement.

According to cell-based data, (*R*)-4′-methylklavuzon inhibits endogenous class I/II HDAC enzymes. But both *in vitro* class I/II HDAC enzyme activity measurement and *in vitro* HDAC1 enzyme activity measurement showed that (*R*)-4′-methylklavuzon does not have significant inhibitory effects on HDAC enzymes. However, *in vitro* SIRT1 enzyme activity measurement showed that 100 μM of (*R*)-4′-methylklavuzon already inhibits SIRT1 activity by half. This data supports that inhibition obtained from cell-based HDAC enzymatic activity measurement might have been achieved by sirtuin inhibition rather than HDAC inhibition because tested substrate (Boc-Lys (Ac)-7-Amino-4-Methylcoumarin (Boc-Lys (Ac)-AMC)) can also be deacetylated by sirtuins [64–66].

(*R*)-4′-methylklavuzon increased the ratio of reactive oxygen species in HuH-7 parental cells at 1.0 μM concentration after 24 h of drug administration. It is known that SIRT1 is involved in DNA repair mechanism which can be triggered by genotoxicity or accumulation of reactive oxygen species [67,68]. ELISA assays showed (*R*)-4′-methylklavuzon upregulates intracellular SIRT1 protein levels in parental cells dose dependently except 5.0 μM which is lethal dose after 24 h. We can also emphasize that SIRT1 protein levels were increased 3.3, 3.9 and 2 times at 1.0, 3.0 and 5.0 μM concentrations compared to the untreated cells, respectively. Comparison of cell-based Sirtuin/HDAC enzyme activity inhibition and endogenous SIRT1 protein levels provided a supporting evidence for endogenous SIRT1 inhibition inside the cells. Although SIRT1 protein levels were significantly upregulated at the abovementioned concentrations, endogenous Sirtuin/HDAC enzyme activity was decreased at the same concentrations after 24 h (Fig. 4D).

(*R*)-4′-methylklavuzon significantly overexpresses intracellular SIRT1 protein levels. This overexpression might be a result of DNA break formation, increased reactive oxygen species or topoisomerase I inhibition by (*R*)-4′-methylklavuzon. Inhibition of basal SIRT1 enzyme activity might also be a consequence of this overexpression.

Studies show that there are still conflicting reports for the upregulation or downregulation status of SIRT1 even in the same type of cancer tissues such as breast, colon, gastric and liver [69–74]. Chen et al. showed that SIRT1 was upregulated in a subset of HCC tissues while Wang et al. revealed that SIRT1 was downregulated in HCC [74,75]. Tumor suppressive effect of SIRT1 overexpression was demonstrated in various types of cancers like gastric and colon cancer. Zhang et al. showed that SIRT1 is downregulated in gastric cancer and ectopic overexpression of SIRT1 increased G1 phase arrest and apoptosis [73]. Kabra et al. demonstrated that SIRT1 is overexpressed in approximately 25% of stage I/II/III colorectal adenocarcinomas and rarely overexpressed in stage IV tumors. They also revealed that approximately 30% of colon carcinomas have lower SIRT1 expression compared to normal parenchyma. In this study, they found that SIRT1 overexpression reduces tumor formation. Paradoxically, they showed that pharmacological inhibition of SIRT1 sensitizes cells to apoptosis by chemotherapeutic drugs [72]. In 2011, Chen et al. revealed that SIRT1 mRNA levels between HCC and non-tumoral tissues do not differ but nuclear SIRT1 protein is overexpressed in 46 of 150 HCC tissue samples, which accounts for approximately 30% of the collection. Difference in mRNA and protein levels in HCC samples indicate that SIRT1 is post-transcriptionally overexpressed in HCC. In 2012, Chen et al. showed that SIRT1 is overexpressed in 95 of 172 HCC samples accounting for 50% of the collection. They revealed that SIRT1 protein is regulated by 26S proteasome in a ubiquitin dependent manner. Although SIRT1 is overexpressed in HCC tissues, (*R*)-4′-methylklavuzon might have inhibited deacetylase enzymatic activity of SIRT1, which was shown to be responsible of HCC tumorigenesis. The other reason of SIRT1 overexpression after drug treatment might be an interference in proteasomal degradation by drug candidate. Therapeutic effects of (*R*)-4′-methylklavuzon via SIRT1 overexpression might still be useful for other subtypes of HCC or other cancers (gastric and colon) in which SIRT1 is downregulated.

When DNA damage occurs, cells epigenetically silence damaged region to prevent incorrect gene expression. One of the silencing mechanisms is the upregulation of H3K27me3 by EZH2 which is the only known methyl transferase of H3K27 residue [76]. (*R*)-4′-methylklavuzon was found to upregulate H3K27me3 expression in both HuH-7 parental and EpCAM$^+$/CD133$^+$ cancer stem cells which were sorted by fluorescence-activated cell sorting (FACS) (Fig. 4E).

2.4. TK126 inhibits proliferation of HCC cell lines

In our previous study, novel derivative of (*R*)-4′-methylklavuzon, TK126, showed superior cytotoxic effect on pancreatic cancer cell line Mia-PaCa2 with its low IC_{50} value of 0.16 ± 0.03 μM concentration [41]. We also tested effect of TK126 on the proliferation of HuH-7 and HepG2 cells. According to MTT cell viability assay, IC_{50} values of TK126 were found as 5.0 μM for 24 h, 2.5 μM for 48 h and 1.25 μM for 72 h in HuH-7 parental cells (Fig. 5A). HepG2 cells were slightly sensitive to TK126 with IC_{50} values of 5.0 μM for 24 h, 0.625 μM for 48 h and 0.1 μM for 72 h. TK126 showed similar IC_{50} values like its lead molecule (*R*)-4′-methylklavuzon on HuH-7 cells but it was more effective on HepG2 cells with its IC_{50} value of 0.625 μM and 0.10 μM after 48 and 72 h, respectively (Fig. 5A).

According to literature, goniothalamin has similar IC_{50} values on hepatocellular carcinoma and hepatoblastoma cell lines. It was reported as $IC_{50} = 1.6$ μM on HepG2 and $IC_{50} = 5.4$ μM on Hep3B. In a different study, IC_{50} values of goniothalamin were calculated as 9.2, 8.3 and 4.6 μM at the incubation times of 24, 48 and 72 h, respectively. It is obvious that both (R)-4′-methylklavuzon and TK126 are more effective small molecules compared to goniothalamin on HepG2 cell line with calculated IC_{50} values ranging between 0.625, 1.25 and 2.5 μM at 48 and 72 h of incubation times [2,77].

Various studies showed that FDA-approved drugs, sorafenib and regorafenib tended to show moderate IC_{50} values on HepG2 cells. Compared with the IC_{50} values of (R)-4′-methylklavuzon and TK126 on HepG2, both small molecules tended to have more efficient cytotoxic activities than sorafenib and regorafenib *in vitro* with their lower IC_{50} values [78–82].

Docking of TK126 in SIRT1 enzyme catalytic site was more spontaneous than (*R*)-4′-methylklavuzon with a higher binding score (Fig. 5B). It was also found that 10 and 100 μM of TK126 inhibited 17% and 65% of SIRT1 enzyme activity *in vitro*, respectively (Fig. 5B). Of note, 100 μM of TK126 showed higher inhibitory effect compared to the inhibition achieved by the same concentration of (*R*)-4′-methylklavuzon.

Docking studies confirmed that (*R*)-4′-methylklavuzon and TK126 spontaneously interact with SIRT1 enzyme catalytic site. It was found that (*R*)-4′-methylklavuzon and TK126 inhibit SIRT1 enzyme activity in a dose dependent manner *in vitro*. Sirtuins

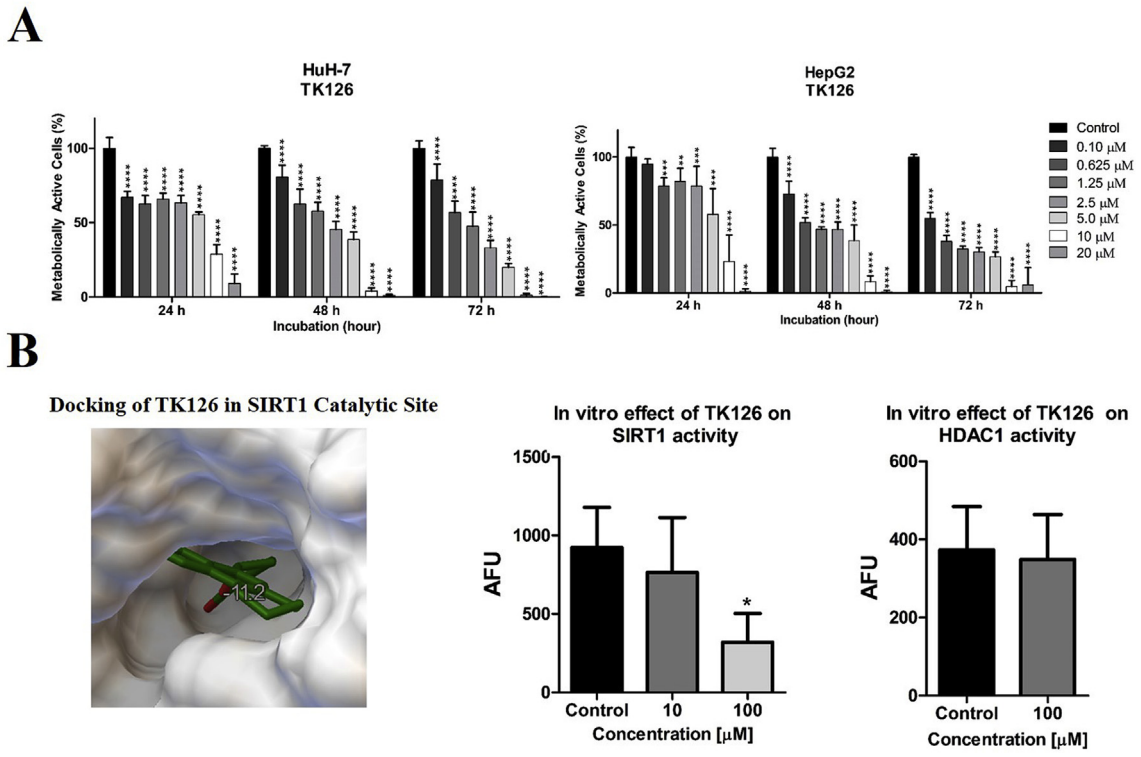

Fig. 5. (**A**) Cytotoxicity analysis of TK126 on HuH-7 parental and HepG2 cells, (**B**) *In silico* docking analysis of TK126 in SIRT1 enzyme catalytic site, Inhibition of SIRT1 enzyme by TK126, Non-inhibitory effects of TK126 on HDAC1 enzyme *in vitro*. Statistical analysis was performed with one-way ANOVA and p-values are <0.001 in ****, <0.001 in ***, <0.01 in ** and <0.05 in * indicating that results are statistically significant.

contain highly conserved residues in their catalytic site or NAD^+ binding site [83]. Inhibition of SIRT1 by drug candidates might be indicative of inhibiting other sirtuin enzymes due to amino acid sequence similarity. This inhibition might have been caused by conformational alterations in SIRT1 protein via docking of drug candidates to catalytic site or interactions of drug candidates with cysteines (Cys371, Cys374, Cys395, Cys398) in Zn^{2+} tetrathiolate subdomain resulting in disruption of Zn^{2+} ion coordination.

Patients with high SIRT1 protein levels show chemoresistance to drugs [50,84]. Oncogenic roles of SIRT1 can be decelerated via inhibition of its enzymatic activity by (*R*)-4′-methylklavuzon and TK126. According to literature, (*R*)-4′-methylklavuzon and TK126 have a chance to reduce this resistance against chemotherapy and sensitize cancer cells for other chemotherapeutical combinations. It was reported that overexpression of SIRT1 attenuates p53-mediated apoptosis which is caused by DNA damage and oxidative stress resulting in cancer cell survival [85]. (*R*)-4′-methylklavuzon inhibits enzymatic activity of overexpressed SIRT1 protein resulting in a decrement in cancer cell proliferation which might be achieved probably by an interference in DNA repair mechanism ability of SIRT1.

2.5. (*R*)-4′-methylklavuzon inhibits CRM1 resulting in RIOK2 and p53 nuclear retention in HCC cell lines

(*R*)-4′-methylklavuzon is structurally similar to goniothalamin which is a CRM1 inhibitor. Previously it was shown by our group that drug candidate inhibits CRM1 mediated nuclear export of RIOK2 (Serine/threonine-protein kinase RIOK2) in HeLa cells. Data revealed that drug candidate starts to inhibit CRM1 at 0.2 μM concentration even at the end of 90 min of incubation and it almost inhibits CRM1 completely in all cells at 50 nM concentration [41].

Similarly, we tested CRM1-inhibitory properties of drug candidate on HepG2 cells. Firstly, cytotoxic effects of (*R*)-4′-methylklavuzon was tested on HepG2 cells and found more effective compared to HuH-7 cells after 24 h of incubation (Fig. S3). Accumulation of RIOK2 in the nucleus is the indication of CRM1 inhibition in the cell. (*R*)-4′-methylklavuzon inhibits CRM1 in HepG2 cells after 6 h at all tested concentrations and maintains this inhibition at 1.00 and 10 μM concentrations after 24 h (Fig. 6 and Fig. S4). Inhibitions of CRM1 in HepG2 cells were also observed after TK126 treatment (Fig. S5). Similar inhibitory effects of (*R*)-4′-methylklavuzon (Figs. S6 and S7) and TK126 (Fig. S8) for CRM1 inhibition were obtained in HuH-7 cells.

We tested outcomes of SIRT1 and CRM1 inhibitions on p53 activity and localization as a mechanism of action that triggers cancer cell death. HepG2 cells were tested due to their low levels of basal p53 protein levels to indicate difference between drug treated and control cells [86]. Significant upregulation in p53 protein levels was achieved at all tested concentrations at the intervals of 6 and 24 h of incubation in HepG2 cells (Fig. 6). Overexpressed p53 protein was observed to be accumulated mainly in the nucleus rather than cytoplasm or entire cell as a result of CRM1 inhibition. Slight upregulation of p53 was also obtained in HuH-7 cells (Fig. S9).

CRM1-inhibitory properties of (*R*)-4′-methylklavuzon and TK126 in HuH-7 and HepG2 cells were shown for the first time with this study. As a result of CRM1 inhibition, RIOK2 was accumulated in nucleus. RIOK2 is considered to play important roles in G2/M transition and it was reported that prolonged mitotic exit was detected when RIOK2 was overexpressed [59]. G2 arrests in HuH-7 cell populations might have been caused by RIOK2 accumulation in nucleus.

We also tested effects of drug candidates and goniothalamin on 3D HepG2 spheroids which were formed in medium by using

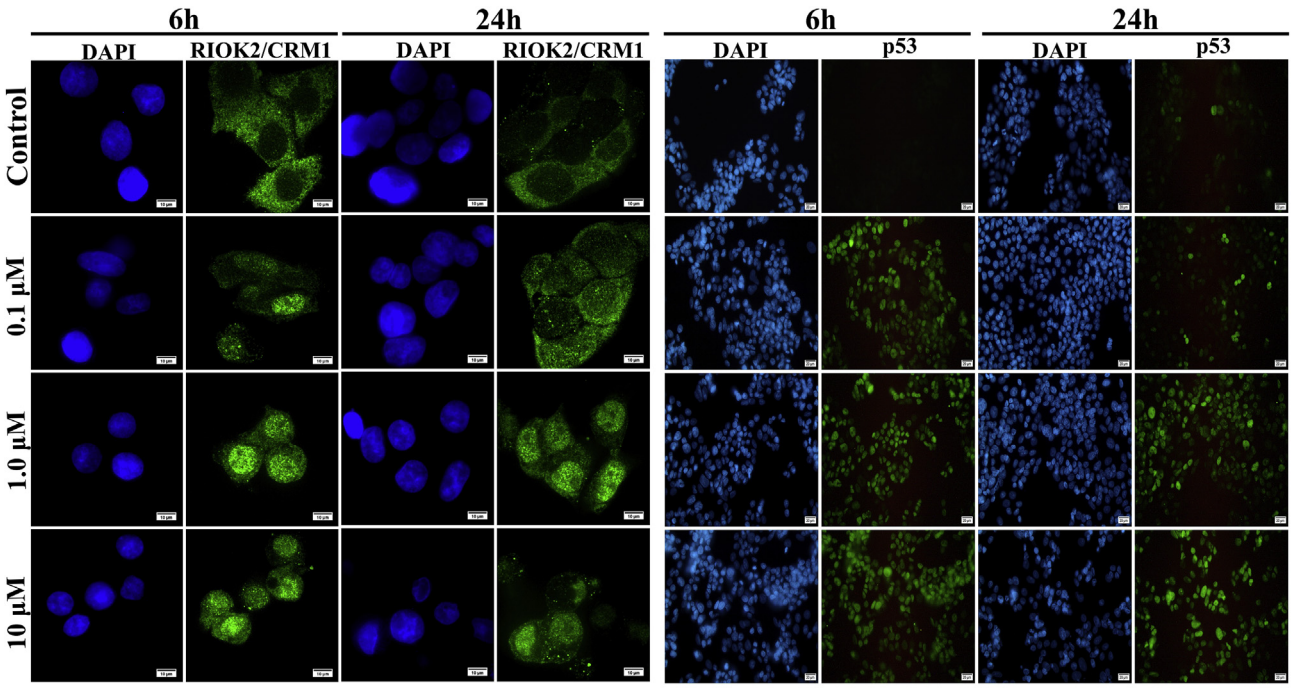

Fig. 6. Spinning disc confocal microscopy imaging of RIOK2 retention in nuclei of HepG2 cells after (*R*)-4′-methylklavuzon treatment indicating CRM1 inhibition. Fluorescence microscopy imaging of p53 in HepG2 cells showing p53 upregulation and nuclear accumulation. Images related to CRM1 inhibition were obtained by using 100X objective with 10 μm scale and images related to p53 upregulation and nuclear retention were obtained by 40X objective with 20 μm scale.

hanging drop method without matrigel. Significant upregulation in p53 protein levels was obtained dose dependently. Propidium iodide (PI) staining revealed that 3D spheroids undergo apoptosis at all tested concentrations of the molecules except 0.1 μM of (*R*)-4′-methylklavuzon. 10 μM of (*R*)-4′-methylklavuzon and TK126 are equally efficient to 50 μM of goniothalamin. Increase in the p53 protein levels and propidium iodide DNA staining was correlated. Drug candidates killed 3D HepG2 spheroids within 24 h although there was no decrement in spheroid volumes (Fig. 7).

Overexpression and stabilization of p53 in cancer patients are one of the most leading therapeutic targets due to their strong tumor suppressive ability. (*R*)-4′-methylklavuzon slightly triggers p53 overexpression in HuH-7 parental cells while it significantly triggers p53 overexpression in HepG2 cells at a lower concentration within a shorter period of time. Moreover, it significantly upregulates p53 protein in HepG2 spheroids in a dose dependent manner resulting in spheroid death according to propidium iodide staining which indicates penetration of drug candidate into entire spheroid. TK126 also shows similar effects on HepG2 spheroids. This data might have been achieved due to a possible DNA damage caused by drug candidate. It was previously showed by our group that (*R*)-4′-methylklavuzon forms comet (DNA breaks) in Mia-PaCa2 cells [41]. Transcriptional activity of p53 is silenced by SIRT1 via deacetylation [87,88]. In addition to p53-regulatory property of HDAC1, SIRT1 is considered to play a crucial role in deacetylation of p53 in cytoplasm whereas HDAC1 deacetylates p53 mostly in nucleus [88,89].

We propose two possible simultaneous mechanism of action related to (*R*)-4′-methylklavuzon and TK126 illustrated in Fig. 7. In cancer cells, SIRT1 is overexpressed and removes acetyl group at Lys382 of p53 protein resulting in an accumulation of p53 in the cytoplasm. Accumulated p53 is transported to mitochondria and it triggers cytochrome *c* release causing p53 transcription-independent apoptosis. When SIRT1 is inhibited, acetyl group at Lys382 is maintained and p53 enters nucleus to transcribe its related tumor suppressor genes like p21 which directs cancer cells

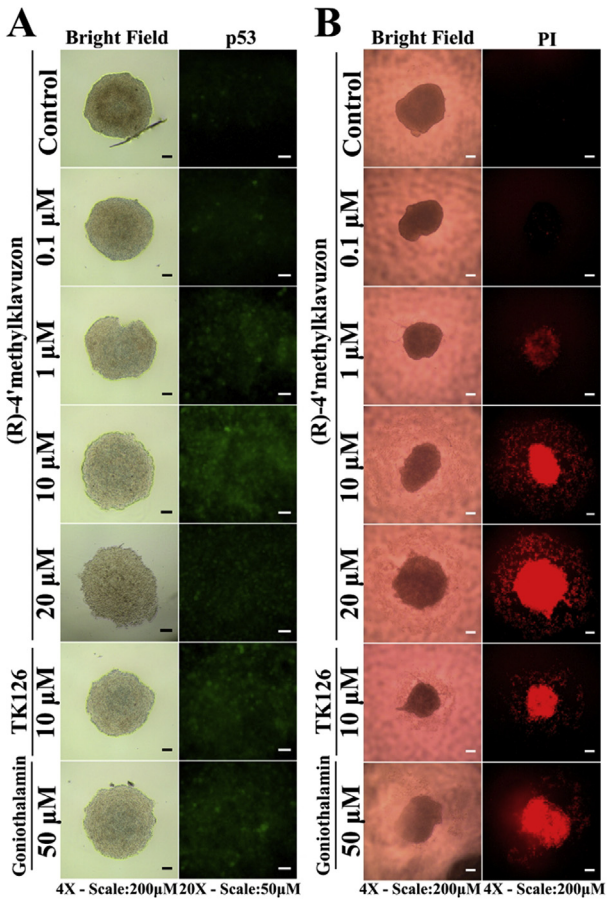

Fig. 7. Microscope images of 3D HepG2 spheroids stained with p53 antibody (**A**) and PI (**B**) after treatment at the end of 24 h of incubation.

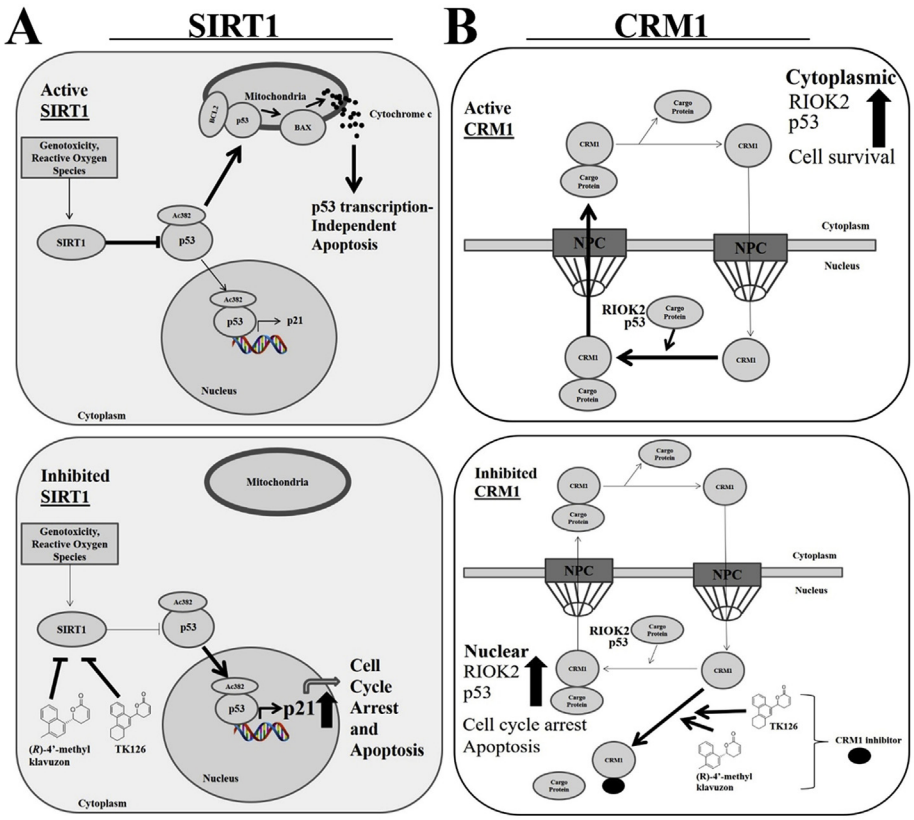

Fig. 8. Mechanism of action underlying G1 arrest caused by (*R*)-4′-methylklavuzon. (**A**) p53 enters nucleus and activates its target genes like p21 for DNA repair, cell cycle arrest or apoptosis when acetylated at the Lys382 residue. When SIRT1 deacetylates p53 at the Lys382 residue, it cannot enter nucleus and it accumulates in cytoplasm followed by transport to mitochondria resulting in p53 transcription-independent apoptosis via cytochrome *c* release. Inhibition of SIRT1 by (*R*)-4′-methylklavuzon and TK126 results in entrance of p53 into nucleus and overexpression of p21 causing cell cycle arrest [90], (**B**) CRM1 transports cargo proteins like RIOK2 and p53 from nucleus to cytoplasm. Aberrant transportation of related proteins causes increased cytoplasmic RIOK2 and p53 levels. Inhibition of CRM1 by (*R*)-4′-methylklavuzon and TK126 results in increased nuclear RIOK2 and p53 levels.

to cell cycle arrests and apoptosis (Fig. 8A). CRM1 is overexpressed in many cancer cells and causes aberrant transportation of various cargo proteins (p21, p53 and SIRT1) and RNA molecules from nucleus to cytoplasm preventing tumor suppressor proteins to play their roles in apoptosis. When CRM1 is inhibited, cargo proteins (p21, p53 and SIRT1) are not exported and retained in nucleus providing their influence in the apoptosis of cancer cells (Fig. 8B).

3. Conclusion

HCC is the second leading cause of death among other cancers and FDA approved drugs such as sorafenib and regorafenib do not cure patients efficiently. It is an urgent need to find novel drug candidates to treat HCC. Here, we proposed (*R*)-4′-methylklavuzon and its derivative TK126 as drug candidates to kill both HCC cells and cancer stem cells.

(*R*)-4′-methylklavuzon was previously synthesized by our group and its cytotoxic effects were demonstrated on prostate, colon, pancreatic, breast, ovary cancer cells [39,41,91,92]. (*R*)-4′-methylklavuzon was also found to irreversibly inhibit topoisomerase I enzyme [39]. Topoisomerases which are classified by Topo I and Topo II, are responsible for regulating DNA topology by forming single or double strand breaks, respectively. Topoisomerase I is overexpressed in liver cancer tissue compared to non-cancerous tissue. Topoisomerase I was reported as an oncogene in HCC and could be used as a biomarker to predict prognosis of the liver cancer patients for efficient treatment options [93]. In this study, we tested growth inhibitory properties of (*R*)-4′-methylklavuzon on HCC cells and HuH-7 EpCAM^{+}/CD133^{+} cancer stem cells by starting the first step to identify possible mechanism of action which is not known yet. Our previous data revealed that (*R*)-4′-methylklavuzon causes G1 and G2 arrests in cancer cells dose dependently [41]. The investigation for mechanism of action related to G1 phase accumulating property of (*R*)-4′-methylklavuzon was the starting point of this study to identify roles of possible players such as class I/II histone deacetylases and class III histone deacetylases called sirtuin enzymes. Another (*R*)-4′-methylklavuzon derivative, TK126 was also tested for growth inhibitory effects on HCC cell lines and it was examined for inhibition of SIRT1 enzyme.

Histone deacetylases (HDAC) which are responsible for the removal of acetyl groups from histone proteins are overexpressed in various types of cancer followed by the downregulation of tumor suppressor genes. Re-acetylation of the chromatin and upregulation of the tumor suppressor genes by inhibiting overexpressed HDAC activity are one of the main therapeutic strategies against cancer.

Class III histone deacetylases, sirtuins, are novel therapeutic targets due to their high occurrence in various diseases such as cancer and Huntington's disease. Sirtuins deacetylate transcription factor p53 resulting in its downregulation. Targeting SIRT1 inhibition is a new alternative to treat related cancers by upregulating p53 levels or stability in cancer cells followed by p53-dependent apoptosis. Inhibition or activation of sirtuins may be useful for treatment according to the sirtuin expression status in the disease.

The role of sirtuins is still an unknown area caused by their function as either tumor-promoter or tumor-suppressor according to cell types and pathways involved. Sirtuin inhibitors will provide us both therapeutic agents and knowledge about mechanism of action.

(*R*)-4′-methylklavuzon and TK126 inhibited proliferation of HCC cell lines, HuH-7 and HepG2 in a dose dependent manner. Additionally, (*R*)-4′-methylklavuzon inhibits proliferation of HuH-7 EpCAM$^+$/CD133$^+$ cancer stem cells by half although they have resistance against anti-cancer molecules. HuH-7 EpCAM$^+$/CD133$^+$ cancer stem cells showed twice fold resistance against (*R*)-4′-methylklavuzon compared to HuH-7 parental cells. Possible reason of this situation might be that ABC-transport proteins in cell plasma membrane are overexpressed in cancer stem cells compared to HuH-7 parental cells [31]. (*R*)-4′-methylklavuzon simultaneously kills HCC cells (HuH-7 and HepG2) and HuH-7 EpCAM$^+$/CD133$^+$ cancer stem cells providing an opportunity to prevent recurrence.

Besides role of SIRT1 in DNA repair mechanism, topoisomerases are important factors in DNA repair. In house experiments showed that (*R*)-4′-methylklavuzon inhibits topoisomerase I which means an interference in DNA repair mechanism [39]. Another apoptosis regulator, E2F1 is known to provoke apoptosis as a consequence of DNA damage. E2F1 is downregulated via deacetylation by SIRT1 [94]. Inductive effects of drug candidate on E2F1 should be investigated as a future perspective.

According to our data in this study, SIRT1 enzyme was inhibited and SIRT1 protein levels were significantly upregulated by (*R*)-4′-methylklavuzon. In addition to possible DNA damage, p53 levels might have been stabilized or increased due to SIRT1 inhibition in HepG2 cells as well. When SIRT1 is inhibited, p53 cannot be deacetylated by SIRT1 and ubiquitinated by MDM2 ligase. As a result of blockage in ubiquitination, p53 cannot be directed to proteasomal degradation and it is maintained in the cell.

It is reported that loss of SIRT1 activity shows cytotoxic effect on HCC cells as a result of G1 arrest [49]. We also found that (*R*)-4′-methylklavuzon causes G1 arrest in both HCC parental cells and HuH-7 EpCAM$^+$/CD133$^+$ cancer stem cells which is consistent with previous literature data. Cytotoxic effect of (*R*)-4′-methylklavuzon on HCC cells and HuH-7 EpCAM$^+$/CD133$^+$ cancer stem cells might be a result of SIRT1 and CRM1 inhibitions followed by increased p53 stability and activity.

It is known that sirtuin and HDAC inhibitors cause G1 arrest in cancer cells as a result of upregulated p21 which is an inhibitor of CDK 4/6. It was shown that (*R*)-4′-methylklavuzon inhibits endogenous sirtuins and upregulates p21 gene expression. Moreover, it caused increase in G1 arrest in HuH-7 cells and EpCAM$^+$/CD133$^+$ cancer stem cells. This increment may be a result of increased p21 gene expressions.

All this data indicates that (*R*)-4′-methylklavuzon damages DNA and increases oxidative stress in HCC cells resulting in p53 protein upregulation and it simultaneously inhibits topoisomerase I preventing DNA repair mechanism. It also inhibits both SIRT1 and CRM1 preventing deacetylation of p53 and nuclear export of p53, respectively. In conclusion, p53 was upregulated due to a possible DNA damage, it was stabilized by endogenous SIRT1 inhibition resulting in its blockage of proteasomal degradation and maintained in nucleus as a result of CRM1 inhibition. p53 which is accumulated in nucleus binds promoter of p21 and upregulates p21 gene expression resulting in G1 arrest.

It is expected that anti-cancer drugs should eliminate cancer stem cells to prevent recurrence of the cancer tissue in patients. We have shown that (*R*)-4′-methylklavuzon inhibits proliferation of hepatocellular carcinoma cells and EpCAM$^+$/CD133$^+$ cancer stem cells providing a novel drug candidate for the treatment of hepatocellular carcinoma for literature.

4. Experimental

4.1. Cell culture

HuH-7 parental, HuH-7 EpCAM$^+$/CD133$^+$ CSCs, HuH-7 EpCAM$^-$/CD133$^-$ non-CSCs and HepG2 were cultured in DMEM supplemented with 10% heat inactivated FBS, 100 U/ml penicillin, 0.1 mg/ml streptomycin, 2 mM L-glutamine and 1% non-essential amino acids solution in a humidified 5% CO_2 incubator at 37 °C.

4.2. Sorting of cancer stem cells by magnetic cell (MACS)

Cancer stem cells were separated from HuH-7 parental cells by using commercial kits from Miltenyi Biotec which is based on the surface markers called CD133 and EpCAM using specific antibodies. EpCAM$^+$/CD133$^+$ cell population which is considered to be cancer stem cells in HuH-7 cell line was separated from EpCAM$^-$/CD133$^-$ cell population by using magnetic cell separation method. 10×10^7 cells were resuspended in 500 μl of MACS Buffer (5% Fetal Bovine Serum and 2 mM EDTA in 1X PBS) and filtered firstly with 100 μm (BD Falcon, 352360) and then 40 μm sterile filters (BD Falcon, 352340). Filtered cells were centrifuged at 2500 rpm and +4 °C followed by resuspension in 300 μl of MACS buffer and treated with 100 μl of FcR blocking buffer (Miltenyi, 130-059-901) to prevent non-specific bindings. EpCAM-FITC antibody (Miltenyi 130-080-301) was added in a ratio of 1:10 as a final concentration and incubated for 10 min at +4 °C in the dark. After antibody labelling, cells were rinsed twice with MACS buffer and centrifuged at 2500 rpm and +4 °C to remove unbound antibodies. EpCAM labelled cells were resuspended in 300 μl of MACS buffer and then anti-FITC magnetic beads (Miltenyi 130-048-701) were added into the suspension. Cells were incubated with magnetic beads for 12 min in the dark at +4 °C and were rinsed twice with MACS buffer. The cell suspension was loaded on positive separating columns (Miltenyi, 130-042-401) to provide the immobilization of labelled cells in the column while unlabeled cells elute from column.

EpCAM$^-$ cells were loaded onto negative separating columns (Miltenyi, 130-042-901) to sort them from all the remaining EpCAM$^+$ cell population. Cells in the positive selection column were eluted after turning the magnetic field off and washing procedure. Same procedures were performed for CD133 surface marker by using specific antibody (Miltenyi, 130-090-826) and micro beads (Miltenyi, 130-090-855). At the end of the entire protocol, EpCAM$^+$/CD133$^+$ and EpCAM$^-$/CD133$^-$ cell populations were obtained and percentage of the positive and negative cells in entire populations were analyzed using flow cytometer (FACS Canto II, BD). Percentage of positivity and negativity in EpCAM$^+$/CD133$^+$ was 85.9% and 5.3%, respectively. Percentage of positivity and negativity in parental cells was 10.6% and 52.8%, respectively. Percentage of positivity and negativity in EpCAM$^-$/CD133$^-$ cells was 12.4% and 42.9%, respectively. Cells sorted by MACS were used in cell viability, cell cycle analysis, apoptosis analysis, p21/p27 gene expression analysis, cell-based HDAC enzyme activity assay.

4.3. Separation of cancer stem cells by fluorescent activated cell sorting (FACS)

Cells were harvested with trypsin and centrifuged at 1500 rpm and +4 °C for 5 min. Cell pellet was washed with 10 ml of FACS buffer (1 mM EDTA, 25 mM HEPES, 1% FBS in PBS). Cells were sequentially filtered with 100 μm (BD Falcon, 352360) and then 40 μm filters (BD Falcon, 352340) to obtain individual cells and then counted. Cells were centrifuged at 1500 rpm and +4 °C for 5 min. Cell pellet was resuspended in FACS buffer and labelled with

EpCAM-FITC antibody (1:11 dilution, Miltenyi 130-080-301) and CD133 antibody (1:11 dilution, Miltenyi 130-090-826). FcR blocking reagent (Miltenyi, 130-059-901) was used to prevent nonspecific bindings. Cells were incubated with abovementioned antibodies at +4 °C for 10 min in the dark. Cells were washed with FACS buffer and centrifuged at 1500 rpm and +4 °C for 5 min to discard unbound antibodies. Pellet was aliquoted as 20 × 106 cells/2 ml in FACS buffer. Cells were labelled with 0.5 μM/ml of DAPI to distinguish live cells. $EpCAM^+/CD133^+$ cells were sorted using flow cytometer (FACS Aria III, BD). Cells sorted by FACS were used in trimethylation analysis of H3K27. Percentage of positive cells were analyzed as 97% after sorting.

4.4. Cell viability assay

2×10^3 cells/well were seeded in 96-well plate and incubated overnight. Cells were treated with 20.00, 10.00, 5.00, 2.50, 1.25, 0.625 and 0.10 μM of (*R*)-4′-methylklavuzon dissolved in DMSO and growth medium for 24, 48 and 72 h. The control cells were treated with only DMSO in 1% final concentration as drug treated cells received. At the end of related intervals, cells were treated with MTT (3-(4,5-dimethylthiazol-2-yl)-2,5-diphenyltetrazolium bromide, Sigma M5655) solution in culture media and further incubated for 4 h at 37 °C in 5% CO_2 incubator. Plates were centrifuged for 10 min at 1800 rpm and medium was removed. 100 μl/well of DMSO was added and plates were shaked orbitally for 15 min. Absorbance measurement was performed at 570 nm with automatic plate reader (Thermo, Varioskan). All experiments were repeated thrice in triplicates.

4.5. Cell cycle analysis

6×10^4 cells/well were seeded in 6-well plates and incubated overnight. Final concentrations of 10.0, 1.0 and 0.1 μM of (*R*)-4′-methylklavuzon that is dissolved in DMSO and growth medium was applied to the cells and incubated for 24, 48 and 72 h. The control cells were treated with only DMSO at 1% final concentration as drug treated cells received. At the end of related intervals, cells were harvested, washed with 1X PBS and centrifuged at 800 rpm for 10 min. Cell pellet was resuspended in 1 ml of 1X ice-cold PBS. Ice-cold absolute ethanol was added dropwise while vortexing. Cells were fixed at −20 °C overnight. After fixation, cells were centrifuged at 1200 rpm for 10 min, washed with ice-cold 1X PBS and centrifuged. Pellet was resuspended in 200 μl of 0.1% Triton X-100 in ice-cold 1X PBS and treated with 20 μL of RNaseA (200 μg/ml) and then incubated at 37 °C under 5% CO_2 for 30 min. Then 20 μL of propidium iodide (1 mg/ml) was added into cell suspensions and incubated for 15 min at room temperature. The percentages of cell cycles were analyzed by a collection of 10000 events using flow cytometer (BD FACS Canto II, BD) and ModFit LT statistics software. Assays were performed in triplicate in parental cells, duplicate in other cell populations.

4.6. Apoptosis analysis

Apoptosis analyses were investigated using Annexin V-FITC (Biovision, K101-100) commercial kit. 6×10^4 cells/well were seeded in 6-well plate and incubated overnight. Cells were treated with 10.0, 1.0 and 0.1 μM concentrations of (*R*)-4′-methylklavuzon that was dissolved in DMSO and growth medium for 24, 48 and 72 h. The control cells were treated with only DMSO at 1% final concentration as drug treated cells received. At the end of related intervals, cells were harvested, washed with ice-cold 1X PBS and centrifuged at 800 rpm at +4 °C for 5 min 250 μL of binding buffer was used to resuspend cell pellet. 2.5 μL of Annexin V-FITC and 2.5 μL of propidium iodide were added and incubated for 5 min in the dark. Apoptosis analysis was performed using flow cytometer (FACS Canto II, BD) and ModFit LT statistics software. Assays were performed in triplicate in parental cells, duplicate in other cell populations.

4.7. Cell-based histone deacetylase enzyme activity measurement using cells sorted by MACS

(*R*)-4′-methylklavuzon was tested on endogenous histone deacetylases inside the hepatocellular carcinoma HuH-7 cell populations by using a commercial kit called cell-based HDAC activity assay kit (Cayman, 600150). Experimental criteria was to maintain equal cell numbers between control and drug-treated populations by using lower concentrations of drug candidate. According to the manufacturer's instructions, 10,000 cells/well were seeded into the black 96-well plates and incubated overnight. 5.00, 3.00, 1.00, 0.50, 0.25 and 0.10 μM concentrations of (*R*)-4′-methylklavuzon were tested on three different cell populations for 24 h. The control cells were treated with only DMSO at 1% final concentration as drug treated cells received. After drug treatment was completed, plate was centrifuged at 500 g for 5 min. Medium was replaced with 200 μL of assay buffer and plate was centrifuged at 500 g for 5 min. Cells were treated with HDAC substrate called Boc-Lys (Ac)-7-Amino-4-Methylcoumarin (Boc-Lys (Ac)-AMC) for 2 h at 37 °C under 5% CO_2. Trichostatin A (TSA) was used as positive control. Lysis/Developer solution was added into each well and fluorescence measurement was performed at 360 excitation wavelenght and 460 emission wavelenght by using a plate reader (Thermo, Varioskan). Results were analyzed using standard curve plotted on a graph. All experiments were repeated in triplicates.

4.8. In vitro SIRT1 enzyme activity measurement

Commercially available fluorescence based SIRT1 Fluorometric Drug Discovery Kit (Enzo, Flour De Lys, BML-AK555) was used to determine inhibitory effects of (*R*)-4′-methylklavuzon on SIRT1 enzyme. The SIRT1 Fluorescent Activity Assay includes Fluor de Lys®-SIRT1 Substrate and Developer II. The Fluor de Lys®-SIRT1 Substrate is a peptide having amino acids 379–382 of human p53 (Arg-His-Lys-Lys (Ac)). The assay's fluorescence signal is generated via deacetylation of the Lys-382 which is an *in vivo* target of SIRT1. In the first step of the procedure, the Fluor de Lys®-SIRT1 Substrate is incubated with human recombinant SIRT1 in the prescence of cosubstrate NAD^+. The substrate is sensitized by deacetylation of Fluor de Lys®-SIRT1 and in the second step, a fluorophore signal is produced via treatment with the Fluor de Lys® Developer II. Resveratrol was used as activator and suramin was used as inhibitor of SIRT1. Effects of (*R*)-4′-methylklavuzon on SIRT1 enzyme activity was tested by combining 1 unit/well of SIRT1 enzyme with 50 μM and 100 μM of drug candidate. SIRT1 was pre-treated with drug candidate before addition of substrate for 2 min. SIRT1 and (*R*)-4′-methylklavuzon were incubated for 1 h at 37 °C with 50 μM of Fluor de Lys Substrate and 500 μM of NAD^+. After incubation, developer solution was added and incubated for 45 min at room temperature. Fluorescence was measured at 360 nm excitation wavelenght and 460 nm emission wavelenght with a plate reader (Thermo, Varioskan). Results were analyzed by using the standard curve plotted on a graph. All experiments were repeated thrice in triplicates.

4.9. Quantification of intracellular SIRT1 levels by ELISA

Intracellular SIRT1 levels in HuH-7 parental cells after (*R*)-4′-methylklavuzon treatment were investigated using a commercially available Sirtuin 1 (human) (IntraCellular) ELISA Kit (Adipogen, AG-

45A-0029YEK-KI01). SIRT1 level was measured based on a sandwich Enzyme Linked-Immunosorbent Assay (ELISA) and monoclonal SIRT1 antibody was precoated onto the 96-well microtiter plate. 5×10^5 Cells were inoculated into tissue culture petri dishes and incubated overnight. 5.00, 3.00 and 1.00 μM concentrations of (*R*)-4′-methylklavuzon were applied to the HuH-7 parental cells and incubated for 24 h. The control cells were treated with only DMSO at 1% final concentration as drug treated cells received. BCA Protein Assay (Pierce, 23227) was used to determine total protein concentration. 44 μg/well cell lysate was added into ELISA plate which is coated with monoclonal SIRT1 antibody and incubated at room temperature. After extensive washing, SIRT1 was detected by a purified polyclonal antibody specific for SIRT1. After excess polyclonal antibody was removed, HRP conjugated anti-rabbit IgG was added and peroxidase activity was measured using the substrate 3,3′,5,5′-tetramethylbenzidine (TMB) at 450 nm on a plate reader (Thermo, MultiSkan). All experiments were repeated thrice in triplicates.

4.10. Spheroid assay based on matrigel

3.76 mg/ml poly-HEMA (Sigma, P3932) in 95% ethanol was used to coat 48-well plates for overnight in incubator at 37 °C and then rinsed with 1X PBS twice. 1000 cells/well were seeded with 2.5 mg/ml matrigel (Corning, 354234) in DMEM. Cell suspensions in 250 μl of matrigel and DMEM mixture were inoculated into four different wells. Plates were centrifuged at 1000 g for 10 min at room temperature and incubated under 37 °C and 5% CO_2 incubator. 350 μl of fresh DMEM medium was added after one day and cells were incubated for four days. Spheroids were treated with only 1% of DMSO as control, 12.5 μM and 62.5 μM of (*R*)-4′-methylklavuzon for 72 h. Microscopic images were obtained at the end of 24, 48 and 72 h by using inverted microscope (Olympus).

4.11. Statistical analysis

Statistical analyses were performed using one-way ANOVA (Analysis of Variance) by GraphPad Prism version 5 (GraphPad Software, San Diego, CA, USA). All drug treated samples were compared versus control groups using Dunnett's multiple comparison test. All data was presented as mean ± SD and p-values less than 0.05 were considered as statistically significant.

Additional methods are given in supplementary material of this manuscript.

Funding sources

This work was supported by The Scientific and Technological Research Council of Turkey [113S464]; IYTE Scientific Research Project [2015-IYTE-04].

Conflicts of interest

The authors declare no competing financial interest.

Acknowledgment

This study was funded by The Scientific and Technological Research Council of Turkey (TUBITAK, project no: 113S464) and Scientific Research Project (2015-IYTE-04). We wish to thank Biotechnology and Bioengineering Application and Research Center (BIYOMER) at IZTECH and Izmir International Biomedicine and Genome Center (IBG) for cancer stem cell sorting, spectrophotometrical and fluorometrical measurements. We also thank Eren Şahin for cancer stem cell sorting by MACS in IBG. We sincerely thank Dr. Özge Tüncel, Dr. Eylem Kurulgan and Prof. Dr. Serdar Özçelik for confocal microscope images.

Appendix A. Supplementary data

Supplementary data to this article can be found online at https://doi.org/10.1016/j.ejmech.2019.07.024.

References

[1] M.A. Seyed, I. Jantan, S.N. Bukhari, Emerging anticancer potentials of goniothalamin and its molecular mechanisms, BioMed Res. Int. 2014 (2014) 536508.
[2] A. de Fatima, L.V. Modolo, L.S. Conegero, R.A. Pilli, C.V. Ferreira, L.K. Kohn, J.E. de Carvalho, Styryl lactones and their derivatives: biological activities, mechanisms of action and potential leads for drug design, Curr. Med. Chem. 13 (2006) 3371–3384.
[3] J.B. Calixto, M.M. Campos, M.F. Otuki, A.R.S. Santos, Anti-inflammatory compounds of plant origin. Part II. Modulation of pro-inflammatory cytokines, chemokines and adhesion molecules, Planta Med. 70 (2004) 93–103.
[4] B.A. Moharam, I. Jantan, J. Jalil, F. Ahmad, Inhibitory effect of compounds from Goniothalamus tapis Miq. And Goniothalamus uvaroides king on Platelet-activating factor receptor binding, Phytother Res. 26 (2012) 687–691.
[5] H.O. Edeoga, D.E. Okwu, B.O. Mbaebie, Phytochemical constituents of some Nigerian medicinal plants, Afr. J. Biotechnol. 4 (2005) 685–688.
[6] M.H. Pan, C.T. Ho, Chemopreventive effects of natural dietary compounds on cancer development, Chem. Soc. Rev. 37 (2008) 2558–2574.
[7] S. AnkiReddy, P. AnkiReddy, G. Sabitha, The first total synthesis of (+)-goniothalesacetate and syntheses of (+)-altholactone, (+)-gonioheptolide A, and (-)-goniofupyrone by an asymmetric acetate aldol approach, Org. Biomol. Chem. 13 (2015) 10487–10495.
[8] D.B. Vendramini-Costa, H.M. Spindola, G.C. de Mello, E. Antunes, R.A. Pilli, J.E. de Carvalho, Anti-inflammatory and antinociceptive effects of racemic goniothalamin, a styryl lactone, Life Sci. 139 (2015) 83–90.
[9] K.K. Kuo, Y.L. Chen, L.R. Chen, C.F. Li, Y.H. Lan, F.R. Chang, Y.C. Wu, Y.L. Shiue, Involvement of phorbol-12-myristate-13-acetate-induced protein 1 in goniothalamin-induced TP53-dependent and -independent apoptosis in hepatocellular carcinoma-derived cells, Toxicol. Appl. Pharmacol. 256 (2011) 8–23.
[10] M. Al-Qubaisi, R. Rozita, S.K. Yeap, A.R. Omar, A.M. Ali, N.B. Alitheen, Selective cytotoxicity of goniothalamin against hepatoblastoma HepG2 cells, Molecules 16 (2011) 2944–2959.
[11] M. Al-Qubaisi, R. Rosli, T. Subramani, A.R. Omar, S.K. Yeap, A.M. Ali, N.B. Alitheen, Goniothalamin selectively induces apoptosis on human hepatoblastoma cells through caspase-3 activation, Nat. Prod. Res. 27 (2013) 2216–2218.
[12] A.M. Alabsi, R. Ali, A.M. Ali, S.A. Al-Dubai, H. Harun, N.H. Abu Kasim, A. Alsalahi, Apoptosis induction, cell cycle arrest and in vitro anticancer activity of gonothalamin in a cancer cell lines, Asian Pac. J. Cancer Prev. APJCP 13 (2012) 5131–5136.
[13] A.M. Alabsi, R. Ali, A.M. Ali, H. Harun, S.A. Al-Dubai, K. Ganasegeran, M.A. Alshagga, S.D. Salem, N.H. Abu Kasim, Induction of caspase-9, biochemical assessment and morphological changes caused by apoptosis in cancer cells treated with goniothalamin extracted from Goniothalamus macrophyllus, Asian Pac. J. Cancer Prev. APJCP 14 (2013) 6273–6280.
[14] S.H. Inayat-Hussain, B.O. Annuar, L.B. Din, A.M. Ali, D. Ross, Loss of mitochondrial transmembrane potential and caspase-9 activation during apoptosis induced by the novel styryl-lactone goniothalamin in HL-60 leukemia cells, Toxicol. Vitro 17 (2003) 433–439.
[15] N. Umar-Tsafe, M.S. Mohamed-Said, R. Rosli, L.B. Din, L.C. Lai, Genotoxicity of goniothalamin in CHO cell line, Mutat. Res. 562 (2004) 91–102.
[16] A.M. Ali, M.M. Mackeen, M. Hamid, Q.B. Aun, Y. Zauyah, H.L. Azimahtol, K. Kawazu, Cytotoxicity and electron microscopy of cell death induced by goniothalamin, Planta Med. 63 (1997) 81–83.
[17] A.H. Pihie, J. Stanslas, L.B. Din, Non-steroid receptor-mediated antiproliferative activity of styrylpyrone derivative in human breast cancer cell lines, Anticancer Res. 18 (1998) 1739–1743.
[18] S.H. Inayat-Hussain, A.B. Osman, L.B. Din, A.M. Ali, R.T. Snowden, M. MacFarlane, K. Cain, Caspases-3 and -7 are activated in goniothalamin-induced apoptosis in human Jurkat T-cells, FEBS Lett. 456 (1999) 379–383.
[19] R.C. Barcelos, J.C. Pastre, D.B. Vendramini-Costa, V. Caixeta, G.B. Longato, P.A. Monteiro, J.E. de Carvalho, R.A. Pilli, Design and synthesis of N-acylated aza-goniothalamin derivatives and evaluation of their in vitro and in vivo antitumor activity, ChemMedChem 9 (2014) 2725–2743.
[20] R.C. Barcelos, K.J. Pelizzaro-Rocha, J.C. Pastre, M.P. Dias, C.V. Ferreira-Halder, R.A. Pilli, A new goniothalamin N-acylated aza-derivative strongly down-regulates mediators of signaling transduction associated with pancreatic cancer aggressiveness, Eur. J. Med. Chem. 87 (2014) 745–758.
[21] M. Bruder, D.B. Vendramini-Costa, J.E. de Carvalho, R.A. Pilli, Design, synthesis and in vitro evaluation against human cancer cells of 5-methyl-5-styryl-2,5-dihydrofuran-2-ones, a new series of goniothalamin analogues, Bioorg. Med. Chem. 21 (2013) 5107–5117.

[22] V.J.N. Bykov, S.E. Eriksson, J. Bianchi, K.G. Wiman, Targeting mutant p53 for efficient cancer therapy, Nat. Rev. Canc. 18 (2018) 89–102.
[23] R. Lillico, N. Stesco, T. Khorshid Amhad, C. Cortes, M.P. Namaka, T.M. Lakowski, Inhibitors of enzymes catalyzing modifications to histone lysine residues: structure, function and activity, Future Med. Chem. 8 (2016) 879–897.
[24] J. Zawacka-Pankau, G. Selivanova, Pharmacological reactivation of p53 as a strategy to treat cancer, J. Intern. Med. 277 (2015) 248–259.
[25] M. Gersch, J. Kreuzer, S.A. Sieber, Electrophilic natural products and their biological targets, Nat. Prod. Rep. 29 (2012) 659–682.
[26] F. Yeung, J.E. Hoberg, C.S. Ramsey, M.D. Keller, D.R. Jones, R.A. Frye, M.W. Mayo, Modulation of NF-kappaB-dependent transcription and cell survival by the SIRT1 deacetylase, EMBO J. 23 (2004) 2369–2380.
[27] N.Y. Song, Y.J. Surh, Janus-faced role of SIRT1 in tumorigenesis, Ann. N. Y. Acad. Sci. 1271 (2012) 10–19.
[28] M. Romano, F. De Francesco, G. Pirozzi, E. Gringeri, R. Boetto, M. Di Domenico, B. Zavan, G.A. Ferraro, U. Cillo, Expression of cancer stem cell biomarkers as a tool for a correct therapeutic approach to hepatocellular carcinoma, Oncoscience 2 (2015) 443–456.
[29] T. Yamashita, M. Forgues, W. Wang, J.W. Kim, Q. Ye, H. Jia, A. Budhu, K.A. Zanetti, Y. Chen, L.X. Qin, Z.Y. Tang, X.W. Wang, EpCAM and alpha-fetoprotein expression defines novel prognostic subtypes of hepatocellular carcinoma, Cancer Res. 68 (2008) 1451–1461.
[30] H. Zheng, Y. Pomyen, M.O. Hernandez, C. Li, F. Livak, W. Tang, H. Dang, T.F. Greten, J.L. Davis, Y. Zhao, M. Mehta, Y. Levin, J. Shetty, B. Tran, A. Budhu, X.W. Wang, Single-cell analysis reveals cancer stem cell heterogeneity in hepatocellular carcinoma, Hepatology 68 (2018) 127–140.
[31] S. Ma, K.W. Chan, T.K. Lee, K.H. Tang, J.Y. Wo, B.J. Zheng, X.Y. Guan, Aldehyde dehydrogenase discriminates the CD133 liver cancer stem cell populations, Mol. Cancer Res. 6 (2008) 1146–1153.
[32] H. Modjtahedi, B.C. Cho, M.C. Michel, F. Solca, A comprehensive review of the preclinical efficacy profile of the ErbB family blocker afatinib in cancer, Naunyn-Schmiedeberg's Arch. Pharmacol. 387 (2014) 505–521.
[33] A. Hamasy, Q. Wang, K.E. Blomberg, D.K. Mohammad, L. Yu, M. Vihinen, A. Berglof, C.I. Smith, Substitution scanning identifies a novel, catalytically active ibrutinib-resistant BTK cysteine 481 to threonine (C481T) variant, Leukemia 31 (2017) 177–185.
[34] L. Wang, J. Zhao, Y. Yao, C. Wang, J. Zhang, X. Shu, X. Sun, Y. Li, K. Liu, H. Yuan, X. Ma, Covalent binding design strategy: a prospective method for discovery of potent targeted anticancer agents, Eur. J. Med. Chem. 142 (2017) 493–505.
[35] K. Feldinger, A. Kong, Profile of neratinib and its potential in the treatment of breast cancer, Breast Canc. 7 (2015) 147–162.
[36] A. Chaikuad, P. Koch, S.A. Laufer, S. Knapp, The cysteinome of protein kinases as a target in drug development, Angew Chem. Int. Ed. Engl. 57 (2018) 4372–4385.
[37] K.M. Backus, Applications of reactive cysteine profiling, in: B.F. Cravatt (Ed.), Activity-Based Protein Profiling, Springer International Publishing, Cham, 2019, pp. 375–417.
[38] M.R. Janes, J. Zhang, L.S. Li, R. Hansen, U. Peters, X. Guo, Y. Chen, A. Babbar, S.J. Firdaus, L. Darjania, J. Feng, J.H. Chen, S. Li, S. Li, Y.O. Long, C. Thach, Y. Liu, A. Zarieh, T. Ely, J.M. Kucharski, L.V. Kessler, T. Wu, K. Yu, Y. Wang, Y. Yao, X. Deng, P.P. Zarrinkar, D. Brehmer, D. Dhanak, M.V. Lorenzi, D. Hu-Lowe, M.P. Patricelli, P. Ren, Y. Liu, Targeting KRAS mutant cancers with a covalent G12C-specific inhibitor, Cell 172 (2018) 578–589 e517.
[39] I. Akcok, D. Mete, A. Sen, P. Kasaplar, K.S. Korkmaz, A. Cagir, Synthesis and Topoisomerase I inhibitory properties of klavuzon derivatives, Bioorg. Chem. 71 (2017) 275–284.
[40] S.M. Lee, W.G. Lee, Y.C. Kim, H. Ko, Synthesis and biological evaluation of alpha,beta-unsaturated lactones as potent immunosuppressive agents, Bioorg. Med. Chem. Lett 21 (2011) 5726–5729.
[41] T. Kanbur, M. Kara, M. Kutluer, A. Sen, M. Delman, A. Alkan, H.O. Otas, I. Akcok, A. Cagir, CRM1 inhibitory and antiproliferative activities of novel 4'-alkyl substituted klavuzon derivatives, Bioorg. Med. Chem. 25 (2017) 4444–4451.
[42] N. Panathur, U. Dalimba, P.V. Koushik, M. Alvala, P. Yogeeswari, D. Sriram, V. Kumar, Identification and characterization of novel indole based small molecules as anticancer agents through SIRT1 inhibition, Eur. J. Med. Chem. 69 (2013) 125–138.
[43] J. Wu, Y. Li, K. Chen, H. Jiang, M.H. Xu, D. Liu, Identification of benzofuran-3-yl(phenyl)methanones as novel SIRT1 inhibitors: binding mode, inhibitory mechanism and biological action, Eur. J. Med. Chem. 60 (2013) 441–450.
[44] K.S. Fritz, J.J. Galligan, R.L. Smathers, J.R. Roede, C.T. Shearn, P. Reigan, D.R. Petersen, 4-Hydroxynonenal inhibits SIRT3 via thiol-specific modification, Chem. Res. Toxicol. 24 (2011) 651–662.
[45] K.S. Kalous, S.L. Wynia-Smith, M.D. Olp, B.C. Smith, Mechanism of Sirt1 NAD+-dependent protein deacetylase inhibition by cysteine S-nitrosation, J. Biol. Chem. 291 (2016) 25398–25410.
[46] L. Liu, C. Liu, Q. Zhang, J. Shen, H. Zhang, J. Shan, G. Duan, D. Guo, X. Chen, J. Cheng, Y. Xu, Z. Yang, C. Yao, M. Lai, C. Qian, SIRT1-mediated transcriptional regulation of SOX2 is important for self-renewal of liver cancer stem cells, Hepatology 64 (2016) 814–827.
[47] H.C. Chen, Y.M. Jeng, R.H. Yuan, H.C. Hsu, Y.L. Chen, SIRT1 promotes tumorigenesis and resistance to chemotherapy in hepatocellular carcinoma and its expression predicts poor prognosis, Ann. Surg. Oncol. 19 (2012) 2011–2019.
[48] L. Li, L. Wang, L. Li, Z. Wang, Y. Ho, T. McDonald, T.L. Holyoake, W. Chen, R. Bhatia, Activation of p53 by SIRT1 inhibition enhances elimination of CML leukemia stem cells in combination with imatinib, Cancer Cell 21 (2012) 266–281.
[49] S. Portmann, R. Fahrner, A. Lechleiter, A. Keogh, S. Overney, A. Laemmle, K. Mikami, M. Montani, M.P. Tschan, D. Candinas, D. Stroka, Antitumor effect of SIRT1 inhibition in human HCC tumor models in vitro and in vivo, Mol. Cancer Ther. 12 (2013) 499–508.
[50] L. Li, T. Osdal, Y. Ho, S. Chun, T. McDonald, P. Agarwal, A. Lin, S. Chu, J. Qi, L. Li, Y.T. Hsieh, C. Dos Santos, H. Yuan, T.Q. Ha, M. Popa, R. Hovland, O. Bruserud, B.T. Gjertsen, Y.H. Kuo, W. Chen, S. Lain, E. McCormack, R. Bhatia, SIRT1 activation by a c-MYC oncogenic network promotes the maintenance and drug resistance of human FLT3-ITD acute myeloid leukemia stem cells, Cell. Stem. Cell. 15 (2014) 431–446.
[51] T.R. Kau, J.C. Way, P.A. Silver, Nuclear transport and cancer: from mechanism to intervention, Nat. Rev. Canc. 4 (2004) 106–117.
[52] J.G. Turner, J. Dawson, D.M. Sullivan, Nuclear export of proteins and drug resistance in cancer, Biochem. Pharmacol. 83 (2012) 1021–1032.
[53] D. Xu, N.V. Grishin, Y.M. Chook, NESdb: a database of NES-containing CRM1 cargoes, Mol. Biol. Cell 23 (2012) 3673–3676.
[54] S. Boyault, D.S. Rickman, A. de Reynies, C. Balabaud, S. Rebouissou, E. Jeannot, A. Herault, J. Saric, J. Belghiti, D. Franco, P. Bioulac-Sage, P. Laurent-Puig, J. Zucman-Rossi, Transcriptome classification of HCC is related to gene alterations and to new therapeutic targets, Hepatology 45 (2007) 42–52.
[55] M. Beck, P. Schirmacher, S. Singer, Alterations of the nuclear transport system in hepatocellular carcinoma - new basis for therapeutic strategies, J. Hepatol. 67 (2017) 1051–1061.
[56] M.E. Barros, J.C. Freitas, J.M. Oliveira, C.H. da Cruz, P.B. da Silva, L.C. de Araujo, G.C. Militao, T.G. da Silva, R.A. Oliveira, P.H. Menezes, Synthesis and evaluation of (-)-Massoialactone and analogues as potential anticancer and anti-inflammatory agents, Eur. J. Med. Chem. 76 (2014) 291–300.
[57] N. LaRonde-LeBlanc, A. Wlodawer, A family portrait of the RIO kinases, J. Biol. Chem. 280 (2005) 37297–37300.
[58] E. Vanrobays, J.P. Gelugne, P.E. Gleizes, M. Caizergues-Ferrer, Late cytoplasmic maturation of the small ribosomal subunit requires RIO proteins in Saccharomyces cerevisiae, Mol. Cell. Biol. 23 (2003) 2083–2095.
[59] T. Liu, M. Deng, J. Li, X. Tong, Q. Wei, X. Ye, Phosphorylation of right open reading frame 2 (Rio2) protein kinase by polo-like kinase 1 regulates mitotic progression, J. Biol. Chem. 286 (2011) 36352–36360.
[60] A. Yanagisawa, H. Kageyama, Y. Nakatsuka, K. Asakawa, Y. Matsumoto, H. Yamamoto, Enantioselective addition of allylic trimethoxysilanes to aldehydes catalyzed by p-tol-BINAP small middle dotAgF, Angew Chem. Int. Ed. Engl. 38 (1999) 3701–3703.
[61] P. Schwab, R.H. Grubbs, J.W. Ziller, Synthesis and applications of RuCl2(CHR')(PR3)2: the influence of the alkylidene Moiety on metathesis activity, J. Am. Chem. Soc. 118 (1996) 100–110.
[62] O. Trott, A.J. Olson, AutoDock Vina, Improving the speed and accuracy of docking with a new scoring function, efficient optimization, and multithreading, J. Comput. Chem. 31 (2010) 455–461.
[63] H. Dai, A.W. Case, T.V. Riera, T. Considine, J.E. Lee, Y. Hamuro, H. Zhao, Y. Jiang, S.M. Sweitzer, B. Pietrak, B. Schwartz, C.A. Blum, J.S. Disch, R. Caldwell, B. Szczepankiewicz, C. Oalmann, P. Yee Ng, B.H. White, R. Casaubon, R. Narayan, K. Koppetsch, F. Bourbonais, B. Wu, J. Wang, D. Qian, F. Jiang, C. Mao, M. Wang, E. Hu, J.C. Wu, R.B. Perni, G.P. Vlasuk, J.L. Ellis, Crystallographic structure of a small molecule SIRT1 activator-enzyme complex, Nat. Commun. 6 (2015) 7645.
[64] J. Seidel, C. Klockenbusch, D. Schwarzer, Investigating deformylase and deacylase activity of Mammalian and bacterial sirtuins, Chembiochem 17 (2016) 398–402.
[65] A. Dose, J.O. Jost, A.C. Spiess, P. Henklein, M. Beyermann, D. Schwarzer, Facile synthesis of colorimetric histone deacetylase substrates, Chem Commun (Camb) 48 (2012) 9525–9527.
[66] M.T. Borra, B.C. Smith, J.M. Denu, Mechanism of human SIRT1 activation by resveratrol, J. Biol. Chem. 280 (2005) 17187–17195.
[67] A. Chalkiadaki, L. Guarente, The multifaceted functions of sirtuins in cancer, Nat. Rev. Canc. 15 (2015) 608–624.
[68] C. O'Callaghan, A. Vassilopoulos, Sirtuins at the crossroads of stemness, aging, and cancer, Aging Cell 16 (2017) 1208–1218.
[69] J.Y. Sung, R. Kim, J.E. Kim, J. Lee, Balance between SIRT1 and DBC1 expression is lost in breast cancer, Cancer Sci. 101 (2010) 1738–1744.
[70] R.H. Wang, Y. Zheng, H.S. Kim, X.L. Xu, L. Cao, T. Luhasen, M.H. Lee, C.Y. Xiao, A. Vassilopoulos, W.P. Chen, K. Gardner, Y.G. Man, M.C. Hung, T. Finkel, C.X. Deng, Interplay among BRCA1, SIRT1, and survivin during BRCA1-associated tumorigenesis, Mol. Cell 32 (2008) 11–20.
[71] W. Stunkel, B.K. Peh, Y.C. Tan, V.M. Nayagam, X. Wang, M. Salto-Tellez, B. Ni, M. Entzeroth, J. Wood, Function of the SIRT1 protein deacetylase in cancer, Biotechnol. J. 2 (2007) 1360–1368.
[72] N. Kabra, Z. Li, L. Chen, B. Li, X. Zhang, C. Wang, T. Yeatman, D. Coppola, J. Chen, SirT1 is an inhibitor of proliferation and tumor formation in colon cancer, J. Biol. Chem. 284 (2009) 18210–18217.
[73] Y.G. Zhang, X.Q. Cai, N. Chai, Y. Gu, S. Zhang, M.L. Ding, H.C. Cao, S.M. Sha, J.P. Yin, M.B. Li, K.C. Wu, Y.Z. Nie, SIRT1 is reduced in gastric adenocarcinoma and acts as a potential tumor suppressor in gastric cancer, Gastrointest Tumors 2 (2015) 109–123.
[74] J. Chen, B. Zhang, N. Wong, A.W.I. Lo, K.F. To, A.W.H. Chan, M.H.L. Ng, C.Y.S. Ho, S.H. Cheng, P.B.S. Lai, J. Yu, H.K. Ng, M.T. Ling, A.L. Huang, X.F. Cai, B.C.B. Ko, Sirtuin 1 is upregulated in a subset of hepatocellular carcinomas where it is essential for telomere maintenance and tumor cell growth, Cancer Res. 71

(2011) 4138–4149.
[75] R.H. Wang, K. Sengupta, C. Li, H.S. Kim, L. Cao, C. Xiao, S. Kim, X. Xu, Y. Zheng, B. Chilton, R. Jia, Z.M. Zheng, E. Appella, X.W. Wang, T. Ried, C.X. Deng, Impaired DNA damage response, genome instability, and tumorigenesis in SIRT1 mutant mice, Cancer Cell 14 (2008) 312–323.
[76] H.M. O'Hagan, H.P. Mohammad, S.B. Baylin, Double strand breaks can initiate gene silencing and SIRT1-dependent onset of DNA methylation in an exogenous promoter CpG island, PLoS Genet. 4 (2008), e1000155.
[77] Q. Mu, W.D. Tang, R.Y. Liu, C.M. Li, L.G. Lou, H.D. Sun, C.Q. Hu, Constituents from the stems of Goniothalamus griffithii, Planta Med. 69 (2003) 826–830.
[78] J.H. Liu, Y.H. Liu, L.Y. Meng, B. Ji, D.Q. Yang, Synergistic antitumor effect of sorafenib in combination with ATM inhibitor in hepatocellular carcinoma cells, Int. J. Med. Sci. 14 (2017) 523–529.
[79] J.C. Wei, F.D. Meng, K. Qu, Z.X. Wang, Q.F. Wu, L.Q. Zhang, Q. Pang, C. Liu, Sorafenib inhibits proliferation and invasion of human hepatocellular carcinoma cells via up-regulation of p53 and suppressing FoxM1, Acta Pharmacol. Sin. 36 (2015) 241–251.
[80] W. Chen, J. Wu, H. Shi, Z. Wang, G. Zhang, Y. Cao, C. Jiang, Y. Ding, Hepatic stellate cell coculture enables sorafenib resistance in Huh7 cells through HGF/c-Met/Akt and Jak2/Stat3 pathways, BioMed Res. Int. 2014 (2014) 764981.
[81] M. Cervello, D. Bachvarov, N. Lampiasi, A. Cusimano, A. Azzolina, J.A. McCubrey, G. Montalto, Molecular mechanisms of sorafenib action in liver cancer cells, Cell Cycle 11 (2012) 2843–2855.
[82] S. Llerena, N. Garcia-Diaz, S. Curiel-Olmo, A. Agraz-Doblas, A. Garcia-Blanco, H. Pisonero, M. Varela, M. Santibanez, C. Almaraz, L. Cereceda, N. Martinez, M.T. Arias-Loste, A. Puente, L. Martin-Ramos, C.R. de Lope, F. Castillo-Suescun, C. Cagigas-Fernandez, P. Isidro, C. Lopez-Lopez, M. Lopez-Hoyos, J. Llorca, J. Aguero, B. Crespo-Facorro, I. Varela, M.A. Piris, J. Crespo, J.P. Vaque, Applied diagnostics in liver cancer. Efficient combinations of sorafenib with targeted inhibitors blocking AKT/mTOR, Oncotarget 9 (2018) 30869–30882.
[83] J.L. Avalos, K.M. Bever, C. Wolberger, Mechanism of sirtuin inhibition by nicotinamide: altering the NAD(+) cosubstrate specificity of a Sir2 enzyme, Mol. Cell 17 (2005) 855–868.
[84] T. Zhang, N.N. Rong, J. Chen, C.W. Zou, H.Y. Jing, X.L. Zhu, W.L. Zhang, SIRT1 expression is associated with the chemotherapy response and prognosis of patients with advanced NSCLC, PLoS One 8 (2013).
[85] J.M. Dai, Z.Y. Wang, D.C. Sun, R.X. Lin, S.Q. Wang, SIRT1 interacts with p73 and suppresses p73-dependent transcriptional activity, J. Cell. Physiol. 210 (2007) 161–166.
[86] B. Bressac, K.M. Galvin, T.J. Liang, K.J. Isselbacher, J.R. Wands, M. Ozturk, Abnormal structure and expression of p53 gene in human hepatocellular carcinoma, Proc. Natl. Acad. Sci. U. S. A. 87 (1990) 1973–1977.
[87] J. Luo, F. Su, D. Chen, A. Shiloh, W. Gu, Deacetylation of p53 modulates its effect on cell growth and apoptosis, Nature 408 (2000) 377–381.
[88] J. Luo, A.Y. Nikolaev, S. Imai, D. Chen, F. Su, A. Shiloh, L. Guarente, W. Gu, Negative control of p53 by Sir2alpha promotes cell survival under stress, Cell 107 (2001) 137–148.
[89] H. Vaziri, S.K. Dessain, E. Ng Eaton, S.I. Imai, R.A. Frye, T.K. Pandita, L. Guarente, R.A. Weinberg, hSIR2(SIRT1) functions as an NAD-dependent p53 deacetylase, Cell 107 (2001) 149–159.
[90] J. Yi, J. Luo, SIRT1 and p53, effect on cancer, senescence and beyond, Biochim. Biophys. Acta 1804 (2010) 1684–1689.
[91] P. Kasaplar, O. Yilmazer, A. Cagir, 6-Bicycloaryl substituted (S)- and (R)-5,6-dihydro-2H-pyran-2-ones: asymmetric synthesis, and anti-proliferative properties, Bioorg. Med. Chem. 17 (2009) 311–318.
[92] P. Kasaplar, O.Y. Cakmak, A. Cagir, Michael acceptor properties of 6-bicycloaryl substituted (R)-5,6-dihydro-2H-pyran-2-ones, Bioorg. Chem. 38 (2010) 186–189.
[93] L.M. Liu, D.D. Xiong, P. Lin, H. Yang, Y.W. Dang, G. Chen, DNA topoisomerase 1 and 2A function as oncogenes in liver cancer and may be direct targets of nitidine chloride, Int. J. Oncol. 53 (2018) 1897–1912.
[94] C.G. Wang, L.H. Chen, X.H. Hou, Z.Y. Li, N. Kabra, Y.H. Ma, S. Nemoto, T. Finkel, W. Gu, W.D. Cress, J.D. Chen, Interactions between E2F1 and SirT1 regulate apoptotic response to DNA damage, Nat. Cell Biol. 8 (2006) 1025–U1109.